1 Title Page

Humans and mice fluctuate between external and internal modes of sensory processing.

Authors:

Veith Weilnhammer[1,2], Heiner Stuke[1,2], Anna-Lena Eckert[1,3,5], Kai Standvoss[1,3,5], Philipp Sterzer[1,3,4,5]

Affiliations:

[1] Department of Psychiatry, Charité-Universitätsmedizin Berlin, corporate member of Freie Universität Berlin and Humboldt-Universität zu Berlin, 10117 Berlin, Germany

[2] Berlin Institute of Health, Charité-Universitätsmedizin Berlin and Max Delbrück Center, 10178 Berlin, Germany

[3] Bernstein Center for Computational Neuroscience, Charité-Universitätsmedizin Berlin, 10117 Berlin, Germany

[4] Berlin School of Mind and Brain, Humboldt-Universität zu Berlin, 10099 Berlin, Germany

[5] Einstein Center for Neurosciences Berlin, 10117 Berlin, Germany

Corresponding Author:

Veith Weilnhammer, Department of Psychiatry, Charité Campus Mitte, Charitéplatz 1, 10117 Berlin, phone: 0049 (0)30 450 517 317, email: veith-andreas.weilnhammer@charite.de

2 Abstract

Perception cycles through periods of enhanced and reduced sensitivity to external information. Here, we asked whether such infra-slow oscillations arise as a noise-related epiphenomenon of limited processing capacity or, alternatively, represent a structured mechanism of perceptual inference. Using two large-scale datasets, we found that humans and mice waver between alternating intervals of externally- and internally-oriented modes of sensory analysis. During external mode, perception was more sensitive to external sensory information, whereas internal mode was characterized by enhanced biases toward perceptual history. Computational modeling indicated that dynamic changes in mode are governed by two interlinked factors: (i), the integration of subsequent stimuli over time and, (ii), infra-slow anti-phase oscillations in the perceptual impact of external sensory information versus internal predictions that are provided by perceptual history. Between-mode fluctuations may benefit perception by enabling the generation of stable representations of the environment despite an ongoing stream of noisy sensory inputs.

3 Introduction

The capacity to respond to changes in the environment is a defining feature of life[1–3]. Intriguingly, the ability of living things to process their surroundings fluctuates considerably over time[4,5]. In humans, perception[6–11], cognition[12] and memory[13] cycle through prolonged periods of enhanced and reduced sensitivity to external information, suggesting that the brain detaches from the world in recurring intervals that last from milliseconds to seconds and even minutes[4,5]. Yet breaking from external information is risky, as swift responses to the environment are often crucial to survival.

Since there is an upper bound on the speed and precision at which neural systems can process sensory signals[5], periodic fluctuations in the ability to parse external information[11,14,15] may arise simply due to bandwidth limitations and noise. From an economic perspective, however, it may even be advantageous to actively reduce the costs of sensory processing by seeking external information only in recurring intervals[5,16], otherwise relying on random or stereotypical responses to the external world.

Beyond the energy budget, spending time away from the ongoing stream of sensory inputs may also reflect a functional strategy that facilitates flexible behavior and learning[17]: Intermittently relying more strongly on information acquired from past experiences may enable agents to build up stable internal predictions about the environment despite an ongoing stream of external information[18].

In this work, we asked whether periodicities in the sensitivity to external information represent an epiphenomenon of unstructured neuro-cognitive noise and limited processing capacity or, alternatively, result from a structured and adaptive mechanism of sensory analysis. Using two large-scale datasets on humans[19] and mice[20], we investigated the behavioral correlates and computational principles of infra-slow fluctuations[11] in perception. When less sensitive to external stimulus information, humans and mice relied more strongly on serial dependencies[21–31], i.e., internal predictions that reflect the auto-correlation of natural

environments[32] and bias perceptual decisions toward preceding choices[28,29,33]. Computational modeling indicated that ongoing changes in perceptual performance may be driven by systematic fluctuations between externally- and internally-oriented modes of sensory analysis.

4 Results

4.1 Human perception fluctuates between epochs of enhanced and reduced sensitivity to external information

We began by selecting 71 studies from the Confidence Database[19] that investigated how human participants (N = 4465) perform binary perceptual decisions (Figure 1A; see STAR Methods section for details on inclusion criteria). As a metric for perceptual performance (i.e., the sensitivity to external sensory information), we asked whether the participant's response and the presented stimulus matched (*stimulus-congruent* choices) or differed from each other (*stimulus-incongruent* choices; Figure 1B and C) in a total of 21.88 million trials.

In a first step, we asked whether the ability to accurately perceive sensory stimuli is constant over time or, alternatively, fluctuates in periods of enhanced and reduced sensitivity to external information. We found perception to be stimulus-congruent in 73.46% ± 0.15% of trials (mean ± standard error of the mean; Figure 2A), which was highly consistent across the selected studies (Supplemental Figure S1A). In line with previous work[8], we found that the probability of stimulus-congruence was not independent across successive trials: At the group level, stimulus-congruent perceptual choices were significantly autocorrelated for up to 15 trials. Autocorrelation coefficients decayed exponentially over time (rate $\gamma = -1.92 \times 10^{-3} \pm 4.5 \times 10^{-4}$, $T(6.88 \times 10^4) = -4.27$, $p = 1.98 \times 10^{-5}$; Figure 2B). Importantly, the autocorrelation of stimulus-congruent perception was not a trivial consequence of the experimental design, but remained significant when controlling for the trial-wise autocorrelation of task difficulty (Supplemental Figure S2A) or the sequence of presented stimuli (Supplemental Figure S2B).

In addition, stimulus-congruence was significantly autocorrelated not only at the group-level, but also in individual participants, where the autocorrelation of stimulus-congruent perception exceeded the respective autocorrelation of randomly permuted data within an interval of 3.24 $\pm$ 2.39 $\times$ 10^{-3} trials (Figure 2C). In other words, if a participant's experience was congruent (or incongruent) with the external stimulus information at a given trial, her perception was more likely to be stimulus-congruent (or incongruent) for approximately 3 trials into the future (see Supplemental Figure S2C for a reproduction of this effect using trial-wise logistic regression).

These results confirm that the ability to process sensory signals is not constant over time, but unfolds in multi-trial epochs of enhanced and reduced sensitivity to external information[8]. As a consequence of this autocorrelation, the dynamic probability of stimulus-congruent perception (i.e., computed in sliding windows of $\pm$ 5 trials; Figure 1C) fluctuated considerably within participants (average minimum: 35.47% $\pm$ 0.22%, maximum: 98.27% $\pm$ 0.07%). In line with previous findings[9], such oscillations in the sensitivity to external information had a power density that was inversily proportional to the frequency in the infra-slow spectrum[11] (power $\sim 1/f^{\beta}$, $\beta = -1.32 \pm 3.14 \times 10^{-3}$, $\mathrm{T}(1.84 \times 10^{5}) = -419.48$, $\mathrm{p} < 2.2 \times 10^{-308}$; Figure 2D). This feature, which is also known as *1/f noise*[34,35], represents a characteristic of ongoing fluctuations in complex dynamic systems such as the brain[36] and the cognitive processes it entertains[9,10,12,37,38].

4.2 Human perception oscillates between external and internal modes of sensory processing

In a second step, we sought to explain why perception cycles through periods of enhanced and reduced sensitivity to external information[4,5]. We reasoned that observers may intermittendly rely more strongly on internal information, i.e., on predictions about the environment that are constructed from previous experiences[18,29].

In perception, one of the most basic internal predictions is instantiated by *serial dependencies* that cause perceptual decisions to be systematically biased toward preceding choices[21–31]. Such effects of perceptual history mirror the continuity of the external world, in which the recent past often predicts the near future[28,29,32,33]. Therefore, as a metric for the perceptual impact of internal information, we computed whether the participant's response at a given trial matched or differed from her response at the preceding trial (*history-congruent* and *history-incongruent perception*, respectively; Figure 1B and C).

Firstly, we ensured that perceptual history played a significant role in perception despite the ongoing stream of external information. With a global average of 52.89% ± 0.12% history-congruent trials, we found a small but highly significant perceptual bias towards preceding experiences ($\beta = 16.37 \pm 1.07$, $T(1.09 \times 10^3) = 15.24$, $p = 1.04 \times 10^{-47}$; Figure 2A) that was largely consistent across studies (Supplemental Figure 1B) and more pronounced in participants who were less sensitive to external sensory information (Supplemental Figure 1C). Logistic regression confirmed the internal information provided by perceptual history made a significant contribution to perception ($\beta = 0.11 \pm 5.8 \times 10^{-3}$, $z = 18.51$, $p = 1.65 \times 10^{-76}$) over and above the ongoing stream of external sensory information ($\beta = 2.2 \pm 5.87 \times 10^{-3}$, $z = 374.64$, $p < 2.2 \times 10^{-308}$; see Supplemental Figure S3A for model comparisons within individual participants).

In addition, we confirmed that history-congruence was not a corollary of the sequence of presented stimuli: History-congruent perceptual choices were more frequent when perception was stimulus-incongruent (56.04% ± 0.19%) as opposed to stimulus-congruent (51.81% ± 0.11%, $\beta = -4.22 \pm 0.2$, $T(8.86 \times 10^3) = -20.67$, $p = 9.1 \times 10^{-93}$; Figure 2A, lower panel). Despite being adaptive in auto-correlated real-world environments[18,32,33,39], perceptual history thus represented a source of error in the randomized experimental designs studied here[23,27–29,40].

Secondly, we asked whether perception cycles through multi-trial epochs during which

perception is characterized by stronger or weaker biases toward preceding experiences. Indeed, in close analogy to stimulus-congruence, history-congruence was significantly autocorrelated for up to 21 trials (Figure 2B). Following a peak at the first trial, the respective autocorrelation coefficients decreased exponentially over time (rate $\gamma = -6.11 \times 10^{-3} \pm 5.69 \times 10^{-4}$, $T(6.75 \times 10^4) = -10.74$, $p = 7.18 \times 10^{-27}$). History-congruence remained significantly autocorrelated when controlling for task difficulty (Supplemental Figure S2A) and the sequence of presented stimuli (Supplemental Figure S2B). In individual participants, the autocorrelation of history-congruence was elevated above randomly permuted data for a lag of $4.87 \pm 3.36 \times 10^{-3}$ trials (Figure 2C), confirming that the autocorrelation of history-congruence was not only a group-level phenomenon.

Thirdly, we asked whether the impact of internal information fluctuates as 1/f noise (i.e., a noise characteristic classically associated with fluctuations in the sensitivity to external information[9,10,12,37,38]). The dynamic probability of history-congruent perception (i.e., computed in sliding windows of $\pm$ 5 trials; Figure 1C) varied considerably over time, ranging between a minimum of 12.89% $\pm$ 0.13% and a maximum 92% $\pm$ 0.13%. In analogy to stimulus-congruence, we found that history-congruence fluctuated as 1/f noise, with power densities that were inversily proportional to the frequency in the infra-slow spectrum[11] (power $\sim 1/f^{\beta}$, $\beta = -1.34 \pm 3.16 \times 10^{-3}$, $T(1.84 \times 10^5) = -423.91$, $p < 2.2 \times 10^{-308}$; Figure 2D).

Finally, we ensured that fluctuations in stimulus- and history-congruence are linked to each other. When perceptual choices were less biased toward external information, participants relied more strongly on internal information acquired from perceptual history (and vice versa, $\beta = -0.1 \pm 8.59 \times 10^{-4}$, $T(2.1 \times 10^6) = -110.96$, $p < 2.2 \times 10^{-308}$). Thus, while sharing the characteristic of 1/f noise, fluctuations in stimulus- and history-congruence were shifted against each other by approximately half a cycle (Figure 2E) and showed an average coherence of $6.49 \pm 2.07 \times 10^{-3}$% (Figure S2F).

In sum, our analyses indicate that perceptual decisions may result from a competition between

external sensory signals with internal predictions provided by perceptual history. Crucially, we show that the impact of these external and internal sources of information is not stable over time, but fluctuates systematically, emitting overlapping autocorrelation curves and antiphase 1/f noise profiles.

These links between stimulus- and history-congruence suggest that the fluctuations in the impact of external and internal information may be generated by a unifying mechanism that causes perception to alternate between two opposing *modes*[17] (Figure 1D): During *external mode*, perception is more strongly driven by the available external stimulus information. Conversely, during *internal mode*, participants rely more heavily on internal predictions that are implicitly provided by preceding perceptual experiences. Fluctuations in mode (i.e., the degree of bias toward external versus internal information) may thus provide a novel explanation for ongoing fluctuations in the sensitivity to external information[4,5,17].

4.3 Internal and external modes of processing facilitate response behavior and enhance confidence in human perceptual decision-making

Alternatively, however, fluctuating biases toward externally- and internally-oriented modes may not represent a perceptual phenomenon, but result from cognitive processes that are situated up- or downstream of perception. For instance, it may be argued that participants may be prone to stereotypically repeat the preceding choice when not attending to the experimental task. Thus, fluctuations in mode may arise due to systematic changes in the level of tonic arousal[41] or on-task attention[42,43]. Since arousal and attention typically link closely with response times[42,44] (RTs), this alternative explanation entails that RTs increase monotonically as one moves away from externally-biased and toward internally-biases modes of sensory processing.

As expected, stimulus-congruent (as opposed to stimulus-incongruent) choices were associated

with faster responses ($\beta = -0.14 \pm 1.61 \times 10^{-3}$, $T(1.99 \times 10^6) = -85.93$, $p < 2.2 \times 10^{-308}$; Figure 2G). Intriguingly, whilst controlling for the effect of stimulus-congruence, we found that history-congruent (as opposed to history-incongruent) choices were also characterized by shorter RTs ($\beta = -9.68 \times 10^{-3} \pm 1.38 \times 10^{-3}$, $T(1.99 \times 10^6) = -7.02$, $p = 2.16 \times 10^{-12}$; Figure 2G).

When analyzing the speed of response against the mode of sensory processing (Figure 2H), we found that RTs were shorter during externally-oriented perception ($\beta_1 = -11.07 \pm 0.55$, $T(1.98 \times 10^6) = -20.14$, $p = 3.17 \times 10^{-90}$). Crucially, as indicated by a quadratic relationsship between the mode of sensory processing and RTs ($\beta_2 = -19.86 \pm 0.52$, $T(1.98 \times 10^6) = -38.43$, $p = 5 \times 10^{-323}$), participants became faster at indicating their perceptual decision when biases toward both internal and external mode grew stronger. This argued against the view that the dynamics of pre-perceptual variables such as arousal or attention provide a plausible alternative explanation for the fluctuating perceptual impact of internal and external information.

Secondly, it may be assumed that participants tend to repeat preceding choices when they are not yet familiar with the experimental task, leading to history-congruent choices that are caused by insufficient training. In the Confidence database[19], training effects were visible from RTs that were shortened by increasing exposure to the task ($\beta = -7.57 \times 10^{-5} \pm 6.37 \times 10^{-7}$, $T(1.8 \times 10^6) = -118.7$, $p < 2.2 \times 10^{-308}$). Intruigingly, however, history-congruent choices became more frequent with increased exposure to the task ($\beta = 3.6 \times 10^{-5} \pm 2.54 \times 10^{-6}$, $z = 14.19$, $p = 10^{-45}$), speaking against the proposition that insufficient training induces seriality in response behavior.

As a third caveat, it could be argued that biases toward internal information reflect a post-perceptual strategy that repeats preceding choices when the subjective confidence in the perceptual decision is low. According to this view, subjective confidence should increase monotonically as biases toward external mode become stronger.

Stimulus-congruent (as opposed to stimulus-incongruent) choices were associated with enhanced confidence ($\beta = 0.04 \pm 1.18 \times 10^{-3}$, $T(2.06 \times 10^6) = 36.71$, $p = 7.5 \times 10^{-295}$; Figure 2I). Yet whilst controlling for the effect of stimulus-congruence, we found that history-congruence also increased confidence ($\beta = 0.49 \pm 1.38 \times 10^{-3}$, $T(2.06 \times 10^6) = 352.16$, $p < 2.2 \times 10^{-308}$; Figure 2I).

When depicted against the mode of sensory processing (Figure 2J), subjective confidence was indeed enhanced when perception was more externally-oriented ($\beta_1 = 92.63 \pm 1$, $T(2.06 \times 10^6) = 92.89$, $p < 2.2 \times 10^{-308}$). Importantly, however, participants were more confident in their perceptual decision for stronger biases toward both internal and external mode ($\beta_2 = 39.3 \pm 0.94$, $T(2.06 \times 10^6) = 41.95$, $p < 2.2 \times 10^{-308}$). In analogy to RTs, subjective confidence thus showed a quadratic relationsship to the mode of sensory processing (Figure 2J), contradicting the notion that biases toward internal mode may reflect a post-perceptual strategy employed in situations of low subjective confidence.

The above results indicate that pre- and post-perceptual phenomena such as arousal and metacognition do not map linearly onto the mode of sensory processing, suggesting that slow fluctuations in the respective impact of external and internal information are most likely to affect perception at an early level of sensory analysis[45,46]. Such low-level processing may integrate perceptual history with external inputs into a decision variable[47] that influences not only perceptual choices, but also downstream functions such as speed of response and subjective confidence.

Consequently, our findings predict that human participants lack full metacognitive insight into how strongly external signals and internal predictions contribute to perceptual decision-making. Stronger biases toward perceptual history thus lead to two seemingly contradictory effects: increased error rates (Figure 2A) and enhanced subjective confidence Figure 2I-J). As a corollary, participants with weaker biases toward perceptual history should be better at judging whether their decisions accurately depict the content of external sensory information.

To test this prediction, we assessed metacognitive performance independently of inter-individual differences in perceptual performance in terms of the M-ratio[48] (meta-d'/d' = 0.85 ± 0.02). Indeed, we found that biases toward internal information (i.e., as defined by the average probability of history-congruence) were indeed stronger in participants with reduced metacognitive efficiency ($\beta = -2.95 \times 10^{-3} \pm 9.81 \times 10^{-4}$, $T(4.14 \times 10^3) = -3$, $p = 2.7 \times 10^{-3}$).

4.4 Mice oscillate between external and internal modes of perceptual decision-making

In a prominent functional explanation for serial dependencies[21–27,30,31,45], perceptual history is cast as an internal prediction that leverages the temporal autocorrelation of natural environments for efficient decision-making[28,29,32,33]. We reasoned that, since this autocorrelation is one of the most basic features of our sensory world, fluctuating biases toward preceding perceptual choices should not be a uniquely human phenomenon.

To test whether externally and internally oriented modes of processing exist beyond the human mind, we analyzed data on perceptual decision-making in mice that were extracted from the International Brain Laboratory (IBL) dataset[20]. Here, we restricted our analyses to the *basic* task[20], in which mice responded to gratings of varying contrast that appeared either in the left or right hemifield of with equal probability. We excluded sessions in which mice did not respond correctly to stimuli presented at a contrast above 50% in more than 80% of trials (see STAR Methods), which yielded a final sample of $N = 165$ adequately trained mice that went through 1.46 million trials.

In line with humans, mice were biased toward perceptual history in $54.03\% \pm 0.17\%$ of trials ($T(164) = 23.65$, $p = 9.98 \times 10^{-55}$; Figure 3A and Supplemental Figure S1D). Perceptual history effects remained significant ($\beta = 0.51 \pm 4.49 \times 10^{-3}$, $z = 112.84$, $p = 0$) when controlling for external sensory information in logistic regression ($\beta = 2.96 \pm 4.58 \times 10^{-3}$,

z = 646.1, p $< 2.2 \times 10^{-308}$; see Supplemental Figure S3C-D for model comparisons and β values computed within individual mice).

In the *basic* task of the IBL dataset[20], stimuli were presented at random in either the left or right hemifield. Stronger biases toward perceptual history should therefore decrease perceptual performance. Indeed, history-congruent choices were more frequent when perception was stimulus-incongruent (61.59% ± 0.07%) as opposed to stimulus-congruent (51.81% ± 0.02%, T(164) = 31.37, p = 3.36×10^{-71}; T(164) = 31.37, p = 3.36×10^{-71}; Figure 3A, lower panel), confirming that perceptual history was a source of error[23,27–29,40] as opposed to a feature of the experimental paradigm. Overall, perception was stimulus-congruent in 81.37% ± 0.3% of trials (Figure 3A).

At the group level, we found significant autocorrelations in both stimulus-congruence (86 consecutive trials) and history-congruence (8 consecutive trials), which remained significant when taking into account the respective autocorrelation of task difficulty and external stimulation (Supplemental Figure 2C-D). In contrast to humans, mice showed a negative autocorrelation coefficient of stimulus-congruence at trial 2. This was due to a feature of the experimental design: Errors at a contrast above 50% were followed by a high-contrast stimulus at the same location. Thus, stimulus-incongruent choices on easy trials were more likely to be followed by stimulus-congruent perceptual choices that were facilitated by high-contrast visual stimuli[20].

The autocorrelation of history-congruence closely overlapped with the human data and decayed exponentially after a peak at the first trial (rate $\gamma = -6.7 \times 10^{-3} \pm 5.94 \times 10^{-4}$, T($3.69 \times 10^{4}$) = −11.27, p = 2.07×10^{-29}; Figure 3B). On the level of individual mice, autocorrelation coefficients were elevated above randomly permuted data within a lag of 4.59 ± 0.06 trials for stimulus-congruence and 2.58 ± 0.01 trials for history-congruence (Figure 3C).

In analogy to humans, mice showed anti-phase 1/f fluctuations in the sensitivity to internal

and external information (Figure 3D-F) and relied more strongly on perceptual history when they were less sensitive to sensory information (and vice versa, $\beta = -0.21 \pm 9.92 \times 10^{-4}$, $T(1.33 \times 10^6) = -212.14$, $p < 2.2 \times 10^{-308}$). This confirmed that both humans and mice show systematic fluctuations between externally- and internally-oriented modes of sensory processing.

Next, we asked how external and internal modes relate to the trial duration (TD, a coarse measure of RT in mice that spans the interval from stimulus onset to feedback[20]). Stimulus-congruent (as opposed to stimulus-incongruent) choices were associated with shorter TDs ($\delta = -262.48 \pm 17.1$, T(164) = -15.35, $p = 1.55 \times 10^{-33}$), while history-congruent choices were characterized by longer TDs ($\delta = 30.47 \pm 5.57$, $T(164) = 5.47$, $p = 1.66 \times 10^{-7}$; Figure 3G).

Across the full spectrum of the available data, TDs showed a linear relationship with the mode of sensory processing, with shorter TDs during external mode ($\beta_1 = -4.36 \times 10^4 \pm 1.27 \times 10^3$, $T(1.24 \times 10^6) = -34.31$, $p = 8.43 \times 10^{-258}$, Figure 3H). However, an explorative post-hoc analysis limited to TDs that differed from the median TD by no more than 1.5 x MAD (median absolute distance[49]) indicated that, when mice enganged with the task more swiftly, TDs did indeed show a quadratic relationship with the mode of sensory processing ($\beta_2 = -2.02 \times 10^3 \pm 835.64$, $T(1.1 \times 10^6) = -2.42$, $p = 0.02$, Figure 3I).

As in humans, it is an important caveat to consider whether the observed serial dependencies in murine perception reflect a phenomenon of perceptual inference, or, alternatively, an unspecific strategy that occurs at the level of reporting behavior. We reasoned that, if mice indeed tended to repeat previous choices as a general response pattern, history effects should decrease during training of the perceptual task. We therefore analyzed how stimulus- and history-congruent perceptual choices evolved across sessions in mice that, by the end of training, achieved proficiency (i.e., stimulus-congruence $\geq 80\%$) in the *basic* task of the IBL dataset[20].

As expected, we found that stimulus-congruent perceptual choices became more frequent

($\beta = 0.34 \pm 7.13 \times 10^{-3}$, $T(8.51 \times 10^3) = 47.66$, $p < 2.2 \times 10^{-308}$; Supplemental Figure S4) and TDs were progressively shortened ($\beta = -22.14 \pm 17.06$, $T(1.14 \times 10^3) = -1.3$, $p < 2.2 \times 10^{-308}$) across sessions. Crucially, the frequency of history-congruent perceptual choices also increased during training ($\beta = 0.13 \pm 4.67 \times 10^{-3}$, $T(8.4 \times 10^3) = 27.04$, $p = 1.96 \times 10^{-154}$; Supplemental Figure S4).

As in humans, longer within-session task exposure was associated with an increase in history-congruence ($\beta = 3.6 \times 10^{-5} \pm 2.54 \times 10^{-6}$, $z = 14.19$, $p = 10^{-45}$) and a decrease in TDs ($\beta = -0.1 \pm 3.96 \times 10^{-3}$, $T(1.34 \times 10^6) = -24.99$, $p = 9.45 \times 10^{-138}$). In sum, these findings strongly argue against the proposition that mice show biases toward perceptual history due to an unspecific response strategy.

4.5 Fluctuations in mode result from coordinated changes in the impact of external and internal information on perception.

The empirical data presented above indicate that, for both humans and mice, perception fluctuates between internal an external modes, i.e., multi-trial epochs that are characterized by enhanced sensitivity toward either internal or external information. Since natural environments typically show high temporal redundancy, previous experiences are often good predictors of new stimuli. Serial dependencies may therefore induce autocorrelations in perception by serving as an internal prediction (or *memory* processes[9,12]) about the environment that actively integrates noisy sensory information over time[50].

To build up these internal predictions, the brain may dynamically update the estimated probability of being in a particular perceptual state from the sequence of preceding experiences[33,45,51]. Since the behavioral data showed high autocorrelation in both history- and stimulus-congruence, we assumed that changes in mode may additionally be driven by ongoing wave-like fluctuations[9,12] in the perceptual impact of external and internal information that occur *irrespective* of the sequence of previous experiences.

Here, we used computational modeling to investigate whether these two factors - (i), the dynamic accumulation of sensory evidence across successive trials and, (ii), ongoing anti-phase oscillations in the impact of external and internal information - may generate the observed fluctuations between internally- and externally-biased modes of processing.

We reasoned that binary perceptual decisions depend on the posterior odds of the two alternative states of the environment that participants learn about via noisy sensory information[51]. Following Bayes Rule, we computed the posterior by combining the sensory evidence available at time-point t (i.e., the log likelihood ratio LLR) with the prior probability ψ:

$$L_t = LLR_t * \omega_{LLR} + \psi_t(L_{t-1}, H) * \omega_\psi \tag{1}$$

We derived the prior probability ψ at timepoint t from the posterior probability of perceptual outcomes at timepoint L_{t-1}. Since a switch between the two sources of sensory information can occur at any time, the effect of perceptual history therefore varies according to both the sequence of preceding experiences and the estimated stability of the external environment (i.e., the *hazard rate* H[51]):

$$\psi_t(L_{t-1}, H) = L_{t-1} + log(\frac{1-H}{H} + exp(-L_{t-1})) - log(\frac{1-H}{H} + exp(L_{t-1})) \tag{2}$$

The LLR was computed by applying a sigmoid sensitivity function defined by parameter α to inputs I (see STAR Methods for detailed equations on humans and mice). To allow for alternating periods of internally- and externally-biased modes of perceptual processing that occur irrespective of the sequence of preceding experiences, we assumed that the relative influences of likelihood and prior show coherent anti-phase fluctuations according to $\omega_{LLR} = amp_{LLR} * sin(f * t) + 1$ and $\omega_\psi = amp_\psi * sin(f * t + \pi) + 1$.

Our above analyses have shown that humans and mice showed significant effects of perceptual history that impaired perfomance in randomized psychophysical experiments[23,27–29,40] (Figure

2A and 3A). We therefore expected that humans and mice underestimated the true hazard rate $\hat{H}$ of the experimental environments (Confidence database[19]: $\hat{H}_{Humans} = 0.5 \pm 1.52 \times 10^{-5}$); IBL database[20]: $\hat{H}_{Mice} = 0.49 \pm 6.47 \times 10^{-5}$). Indeed, when fitting our model to the trial-wise perceptual choices (see STAR methods), we found that the estimated (i.e., subjective) hazard rate H was lower than $\hat{H}$ for both humans (H $= 0.45 \pm 4.8 \times 10^{-5}$, $\beta = -6.87 \pm 0.94$, T(61.87) $= -7.33$, p $= 5.76 \times 10^{-10}$) and mice (H $= 0.46 \pm 2.97 \times 10^{-4}$, $\beta = -2.91 \pm 0.34$, T(112.57) $= -8.51$, p $= 8.65 \times 10^{-14}$).

Across individuals, the estimated hazard rate was negatively correlated to the frequency of history-congruent perceptual choices (humans: $\beta = -11.88 \pm 0.5$, T(4.29×10^3) $= -23.57$, p $= 1.26 \times 10^{-115}$; mice: $\beta = -5.86 \pm 0.65$, T(2.08×10^3) $= -8.95$, p $= 7.67 \times 10^{-19}$). Conversely, the estimated sensitivity toward stimulus information α was positvely correlated to the frequency of stimulus-congruent perceptual choices (humans: $\beta = 8.4 \pm 0.26$, T(4.31×10^3) $= 32.87$, p $= 1.3 \times 10^{-211}$; mice: $\beta = 1.93 \pm 0.12$, T(2.07×10^3) $= 16.21$, p $= 9.37 \times 10^{-56}$).

Simulations from the model (based on the posterior model parameters obtained in humans; see STAR Methods for details) closely matched the empirical results outlined above: Simulated perceptual decisions resulted from a competition of perceptual history with incoming sensory signals (Figure 4A). Stimulus- and history-congruence were significantly auto-correlated (Figure 4B-C), fluctuating in anti-phase as 1/f noise (Figure 4D-F). Simulated posterior certainty[27,28,47] (i.e., the absolute of the posterior log ratio $|L_t|$) showed a quadratic relationsship to the mode of sensory processing (Figure 4H), mirroring the relation of RTs and confidence reports to external and internal biases in perception (Figure 2G-H and Figure 3G-H).

Crucially, the overlap between empirical and simulated data broke down when we removed the dynamic belief updating component (i.e., by setting H to 0.5) or the anti-phase oscillations (by setting amp_{LLR}, amp_{ψ} or both to zero) from the model (Supplemental Figure S5). Likwise, our data could not be reproduced by a reset-rebound-model[52] in which the impact of biases

toward internal predictions are removed in the interval between an error trial and the next correct response[52] (Supplemental Figure S6). Computational modeling therefore confirmed that between-mode fluctuations are best explained by two interlinked processes (Figure 1E): (i), the dynamic accumulation of information across successive trials (i.e., following the estimated hazard rate H) and, (ii), ongoing anti-phase oscillations in the impact of external and internal information (i.e., determined by ω_ψ and ω_{LLR}).

To further probe the validity of our modeling approach, we tested whether posterior model quantities could explain aspects of the behavioral data that the model was not fitted to. Firstly, we predicted that the posterior decision variable L_t should not only encode perceptual choices (i.e., the variable used for model estimation), but also predict the speed of response and subjective confidence[28,47]. Indeed, the estimated trial-wise posterior decision certainty $|L_t|$ correlated negatively with RTs in humans ($\beta = -4.36 \times 10^{-3} \pm 4.64 \times 10^{-4}$, T($1.98 \times 10^6$) $= -9.41$, p $= 5.19 \times 10^{-21}$) and TDs mice ($\beta = -30.18 \pm 0.78$, T(1.24×10^6) $= -38.51$, p $< 2.2 \times 10^{-308}$). Likewise, subjective confidence was positively correlated with the estimated posterior decision certainty in humans ($\beta = 7.63 \times 10^{-3} \pm 8.32 \times 10^{-4}$, T($2.06 \times 10^6$) $= 9.18$, p $= 4.48 \times 10^{-20}$).

Secondly, the dynamic accumulation of information inherent to our model entails that biases toward perceptual history are stronger when the posterior decision certainty at the preceding trial is high[28,29,51]. Due to the link between posterior decision certainty and confidence, we reasoned that confident perceptual choices should be more likely to induce history-congruent perception at the subsequent trial[28,29]. In humans, logistic regression indicated that history-congruence was predicted by the posterior decision certainty $|L_{t-1}|$ ($\beta = 8.22 \times 10^{-3} \pm 1.94 \times 10^{-3}$, z $= 4.25$, p $= 2.17 \times 10^{-5}$) and subjective confidence ($\beta = 0.04 \pm 1.62 \times 10^{-3}$, z $= 27.21$, p $= 4.56 \times 10^{-163}$) at the preceding trial.

5 Discussion

In this work, we have investigated the behavioral and computational characteristics of ongoing fluctuations in perceptual decision-making using two large-scale datasets in humans[19] and mice[20]. Humans and mice cycled through recurring intervals of reduced sensitivity to external sensory information, during which they relied more strongly on perceptual history, i.e., an internal prediction that is provided by the sequence of preceding choices. Computational modeling indicated that these infra-slow periodicities are governed by two interlinked factors: (i), the dynamic integration of sensory inputs over time and, (ii), anti-phase oscillations in the strength at which perception is driven by internal versus external sources of information. These cross-species results therefore suggest that ongoing fluctuations in perceptual decision-making arise not merely as a noise-related epiphenomenon of limited processing capacity, but result from a structured mechanism that oscillates between internally- and externally-oriented modes of sensory analysis.

5.1 Serial dependencies represent a pervasive aspect of perceptual decision-making in humans and mice.

A growing body of literature has highlighted that perception is modulated by preceding choices[21–28,30,31]. Our work provides converging cross-species evidence that such serial dependencies are a pervasive and general phenomenon of perceptual decision-making that occurs in humans and mice (Figures 2-3, Supplemental Figures 1 and 3). While introducing errors in randomized psychophysical designs[23,27–29,40] (Figures 2-3A), we found that perceptual history facilitates post-perceptual processes such as speed of response[39] (Figure 2G) and subjective confidence in humans (Figure 2I).

At the level of individual traits, increased biases toward preceding choices were associated with lower sensitivity to external information (Supplemental Figure 1C-D) and reduced metacognitive efficiency. When investigating how serial dependencies evolve over time, we

observed dynamic changes in strength of perceptual history (Figures 2-3B) that created wavering biases toward internally- and externally-biased modes of sensory processing. Between-mode fluctuations may thus provide a new explanation for ongoing changes in perceptual performance[6–11].

5.2 Fluctations in mode enable the generation of robust internal representations by temporarily disconnecting perception from the ongoing stream of external information.

In computational terms, serial dependencies may leverage the temporal autocorrelation of natural environments[29,45] to increase the efficiency of decision-making[33,40]. Such temporal smoothing[45] of sensory inputs may be achieved by updating dynamic predictions about the world based on the sequence of noisy perceptual experiences[21,29], using algorithms such as Kalman filtering[33], Hierarchical Gaussian filtering[53] or sequential Bayes[24,39,51]. At the level of neural mechanisms, the integration of internal with external information may be realized by combining feedback from higher levels in the cortical hierarchy with incoming sensory signals that are fed forward from lower levels[54].

Is there a computational benefit to be gained from temporalily upregularing biases toward preceding choices (Figure 2-3 B and C), instead of combining them with external sensory information at a constant weight (Supplemental Figure S5)? In their adaptive function for perceptual decision-making, internal predictions critically depend on error-driven learning to remain aligned with the current state of the external environment[55]. Yet when the same network processes external and internal information in parallel, the source of error becomes ambiguous: Ongoing activity may be shaped by either incoming sensory signals that are fed forward from the periphery or, alternatively, by internally-stored predictions about the environment that are fed back form higher cortical levels[17,56].

The perceptual system thus faces the challenge of determining whether errors result from

external input or from internally-stored predictions. Akin to the wake-sleep-algorithm in machine learning[57], this credit assignment problem may be solved by cycling through periods of externally- and internally-biased modes of sensory processing[17]. During internal mode, sensory processing is more strongly constrained by predictive processes that auto-encode the agent's environment. Conversely, during external mode, the network is driven predominantly by sensory inputs[17]. Comparing patterns of activity between the two modes may thus generate an unambiguous error signal that aligns internal predictions with the current state of the environment in iterative test-update-cycles[57].

Beyond the *content* of internal predictions, fluctuations in mode may also help to calibrate metacognitive beliefs about ongoing changes in the *reliability* of decision-relevant information: In the case of parallel processing, suboptimal performance may be caused by misjudging the reliability of external information or, alternatively, by over- and underestimating the reliability of internal predictions. This ambiguity is particularly relevant when agents do not have full insight into the strength at which external and internal sources of information contribute to perceptual inference (i.e., when both internal and external modes increase confidence; Figure 2I-J; Figure 4G-H).

Between-mode fluctuations provide a potential solution to this question: In external mode, perceptual errors can provide an estimate of how reliably external sensory information is transmitted by feedforward processes. During internal mode, in turn, perceptual errors are more reflective of deviations in the strength of feedback that regulates how strongly perception is affected by internal predictions[18]. In the context of serial dependencies, this may help to decide whether an error was caused by over-estimating the precision of incoming sensory information or, alternatively, by reliability of internal predictions provided by perceptual history. On a broader scale, between-mode fluctuations may thus regulate the balance between feedforward versus feedback contributions to perception and thereby play a adaptive role in metacognition and reality monitoring[58].

5.3 Arousal, attentional lapses, insufficient training and metacognitive strategies as alternative explanations for between-mode fluctuations

These functional explanations for external and internal modes share the idea that, in order to form stable internal predictions about the statistical properties of the world (e.g., tracking the hazard rate of the environment) or metacognitive beliefs about processes occuring within the agent (e.g., monitoring ongoing changes in the reliability of feedback and feedforward processing), perception needs to temporalily disengage from the continuous stream of external information. By the same token, they presuppose that fluctuations in mode occur at the level of perception[25,28,45,46], and are not a passive phenomenon that is primarily driven by factors situated up- or downstream of sensory analysis.

First, it may be argued that agents stereotypically repeat preceding choices when less alert. Our analyses address this alternative driver of serial dependecies by building on the association between RTs and arousal[42,44]. We found that RTs do not map linearly onto the mode of sensory processing, but become shorter for stronger biases toward both externally- and internall-oriented mode (Figure 2G-H; Figure 3I). In addition, history-congruent choices became more frequent the longer humans and mice were engaged in the experimental task. These observations argue against the view that biases toward internal mode can be explained solely on the ground of ongoing changes in tonic arousal or fatigue[41].

However, internal modes of sensory processing may also be attributed to attentional lapses[59], which are caused by mind-wandering or mind-blanking and show a more complex relation to RTs[59]: While episodes of mind-blanking are characterized by an absence of subjective mental activity, more frequent misses, a relative increase in slow waves over posterior EEG electrodes and increased RTs, episodes of mind-wandering come along which rich inner experiences, more frequent false alarms, a relative increase of slow-wave amplitudes over frontal electrodes and decreased RTs[59].

Yet in contrast to gradual between-mode fluctuations, engaging in mind-wandering as opposed to on-task attention seems to be an all-or-nothing phenomenon[59]. In addition, internally-biased processing did not increase either false alarms or misses, but induced choice errors through an enhanced impact of perceptual history (Figure 2-4A) that unfolded in alternating *streaks*[9,12] of elevated stimulus- and history-congruence. However, it remains an intruiging question for future research how mind-wandering and -blanking can be differentiated from internally-oriented modes of sensory processing in terms of their phenomenology, behavioral characteristics, neural signatures and noise profiles[10,59].

Second, it may be proposed that humans and mice apply a metacognitive response strategy that repeats preceding choices when less confident about their responses or when insufficiently trained on the task. In humans, however, confidence increased for stronger biases toward both external and internal mode (Figure 2I-J). For humans and mice, history-effects grew stronger with increasing exposure to (and expertise in) the task (Supplemental Figure S4). In addition, the existence of external and internal modes in murine perceptual decision-making (Figure 3) implies that between-mode fluctuations do not depend exclusively on the rich cognitive functions associated with human prefrontal cortex[60].

Finally, our computational modeling results provide further evidence against both of the above caveats: Simulations based on estimated model parameters closely matched the empirical data (Figure 4), reproduced aspects of behavior it was not fitted to (such as trial-wise confidence reports and RTs/TD for human and mice, respectively), and predicted that history-congruent choices occur more frequently after high-confidence trials[28,29]. These findings suggest that perceptual choices and post-perceptual processes such as response behavior or metacognition are jointly driven by a dynamic decision variable[47] that encodes uncertainty[27,28,39] and is affected by ongoing changes in the integration of external versus internal information.

5.4 Flucuations in mode as a driver of 1/f dynamics in perception

Our results thus support the idea that, instead of unspecific effects of arousal, attention, training or metacognitive response stragegies, perceptual choices are shaped by dynamic processes that occur at the level of sensory analysis[25,28,46]: (i), the integration of incoming signals over time and, (ii), ongoing fluctuations in the impact of external versus internal sources of decision-related information. It is particularly interesting that these two model components reprocude the established 1/f characteristic[34,35] of fluctuating performance in perception (see Figure 2-4D and previous work[9,10,12]), since this feature has been attributed to both a memory process[12] (corresponding to model component (i): internal predictions that are dynamically updated in response to new inputs) and wave-like variations in perceptual ressources[9] (corresponding to model component (ii): ongoing oscillations in the impact of internal and external information).

1/f noise is an ubiquitous attribute of dynamic complex systems that integrate sequences of contingent sub-processes[34] and exhibit self-organized criticality[35]. As most real-world processes are *critical*, i.e. not completely uniform (or subcritical) nor completely random (or supercritical)[35,61], the brain may have evolved to operate at a critical point as well[36]: Subcritical brains would be impervious to new inputs, whereas supercritical brains would be driven by noise. The 1/f observed in this study thus provides an intriguing connection between the notion that the brain's self-organized criticality is crucial for balancing network stability with information transmission[36] and the adaptive functions of between-mode fluctuations[17], which we propose to support the build-up of robust internal predictions despite an ongoing stream of noisy sensory inputs.

5.5 Dopamine-dependent changes in E-I-balance as a neural mechanism of between-mode fluctuations

The link to self-organized criticality suggests that balanced cortical excitation and inhibition[62] (E-I), which may enable efficient coding[62] by maintaining neural networks in critical states[63], could provide a potential neural mechanism of between-mode fluctuations. Previous work has proposed that the balance between glutamatergic excitation and GABA-ergic inhibition is regulated by activity-dependent feedback through NMDA receptors[64]. Such NMDA-mediated feedback has been related to the integration of external inputs over time[62] (model component (i), Figure 1E), thereby generating serial dependencies in decision-making[65–68]. Intriguingly, slow neuromodulation by dopamine enhances NMDA-dependent signaling[65,69,70] and oscillates at infra-slow frequencies[71,72] that match the temporal dynamics of between-mode fluctuations observed in humans (Figure 2) and mice (Figure 3). Ongoing fluctuations in the impact of external versus internal information (model component (ii)) may thus by caused by phasic changes in E-I-balance that are induced by dopaminergic neurotransmission.

5.6 Limitations and open questions

In this study, we show that perception is attracted toward preceding choices in mice[20] (Figure 3A) and humans (Figure 2A; see Supplemental Figure S1 for analyses within individual studies of the Confidence database[19]). Of note, previous work has shown that perceptual decision-making is concurrently affected by both attractive and repulsive serial biases that operate on dinstinct time-scales and serve complementary functions for sensory processing[26,73,74]: Short-term attraction may serve the decoding of noisy sensory inputs and increase the stability of perception, whereas long-term repulsion may enable efficient encoding and sensitivity to change[26].

Importantly, repulsive biases operate in parellel to attractive biases[26] and are therefore unlikely to account for the ongoing changes in mode that occur in alternating cycles of

internally- and externally-oriented processing. To elucidate whether attraction and repulsion both fluctuate in their impact on perceptual decision-making will be an important task for future research, since this would help to understand whether attractive and repulsive biases are linked in terms of their computational function and neural implementation[26].

A second open question concerns the neurobiological underpinnings of ongoing changes in mode. Albeit purely behavioral, our results tentatively suggest dopaminergic neuromodulation of NMDA-mediated feedback as one potential mechanism of externally- and internally-biased modes. Since between-mode fluctuations were found in both humans and mice, future studies can apply both non-invasive and invasive neuro-imaging and electrophysiology to better understand the neural mechanisms that generate ongoing changes in mode in terms of neuro-anatomy, -chemistry and -circuitry.

Finally, establishing the neural correlates of externally- an internally-biased modes will enable exiting opportunities to investigate their role for adaptive perception and decision-making. Causal interventions via pharmacological challenges, optogenetic manipulations or (non-)invasive brain stimulation will help to understand whether between-mode fluctuations are implicated in resolving credit-assignment problems[17,75] or in calibrating metacognition and reality monitoring[58]. Addressing these questions may therefore provide new insight into the pathophysiology of hallucinations and delusions, which have been characterized by an imbalance in the impact of external versus internal information[76,77] and are typically associated with metacognitive failures and a departure from consensual reality[77].

6 Methods

6.1 Ressource availability

6.1.1 Lead contact

Further information and requests for resources should be directed to and will be fulfilled by the lead contact, Veith Weilnhammer (veith-andreas.weilnhammer@charite.de).

6.1.2 Materials availability

This study did not generate new unique reagents.

6.1.3 Data and code availability

All custom code and behavioral data are available on https://osf.io/ru78n/. This manuscript was created using the *R Markdown* framework, which integrates all data-related computations and the formatted text within one document. With this, we wish to make our approach fully transparent and reproducible for reviewers and future readers.

6.2 Experimental model and subject details

6.2.1 Confidence database

We downloaded the human data from the Confidence database[19] on 21/10/2020, limiting our analyses to the database category *perception*. Within this category, we selected studies in which participants made binary perceptual decision between two alternative outcomes (see Supplemental Table 1). We excluded two studies in which the average perceptual accuracy fell below 50%. After excluding these studies, our sample consisted of 21.05 million trials obtained from 4317 human participants and 66 individual studies.

6.2.2 IBL database

We downloaded the murine data from the IBL database[20] on 28/04/2021. We limited our analyses to the *basic task*, during which mice responded to gratings that appeared with equal probability in the left or right hemifield. Within each mouse, we excluded sessions in which perceptual accuracy was below 80% for stimuli presented at a contrast $\geq$ 50%. After exclusion, our sample consisted of 14.63 million trials trials obtained from 165 mice.

6.3 Method details

6.3.1 Variables of interest

Primary variables of interest: We extracted trial-wise data on the presented stimulus and the associated perceptual decision. Stimulus-congruent choices were defined by perceptual decisions that matched the presented stimuli. History-congruent choices were defined by perceptual choices that matched the perceptual choice at the immediately preceding trial. The dynamic probabilities of stimulus- and history-congruence were computed in sliding windows of ± 5 trials.

The *mode* of sensory processing was derived by subtracting the dynamic probability of history-congruence from the dynamic probability of stimulus-congruence, such that positive values indicate externally-oriented processing, whereas negativ values indicate internally-oriented processing. When visualizing the relation of the mode of sensory processing to confidence, response times or trial duration (see below), we binned the mode variable in 10% intervals. We excluded bins than contained less than 0.5% of the total number of available data-points.

Secondary variables of interest: From the Confidence Database[19], we furthermore extracted trial-wise confidence reports and resonse times (RTs; if RTs were available for both the perceptual decision and the confidence report, we only extracted the RT associated with the perceptual decision). To enable comparability between studies, we normalized RTs and confidence reports within individual studies using the *scale* R function. If not available for a

particular study, RTs and confidence reports were treated as missing variables. From the IBL database[20], we extracted trial durations (TDs) as defined by interval between stimulus onset and feedback, which respresents a coarse meausure of RT[20].

Exclusion criteria for individual data-points: For non-normalized data (TDs from the IBL database[20]; d-prime, meta-dprime and M-ratio from the Confidence database[19] and simulated confidence reports), we excluded data-points that differed from the median by more than 3 x MAD (median absolute distance[49]). For normalized data (RTs and confidence reports from the Confidence database[19]), we excluded data-points that differed from the mean by more than 3 x SD (standard deviation).

6.3.2 Control variables

Next to the sequence of presented stimuli, we assessed the autocorrelation of task difficulty as an alternative explanation for any autocorrelation in stimulus- and history-congruence. For the Confidence Database[19], task difficulty was indicated by one of the following labels: *Difficulty*, *Difference*, *Signal-to-Noise*, *Dot-Difference*, *Congruency*, *Coherence(-Level)*, *Dot-Proportion*, *Contrast(-Difference)*, *Validity*, *Setsize*, *Noise-Level(-Degree)* or *Temporal Distance*. When none of the above was available for a given study, task difficulty was treated as a missing variable. In analogy to RTs and confidence, difficulty levels were normalized within individual studies. For the IBL Database[20], task difficulty was defined by the contrast of the presented grating.

6.3.3 Autocorrelations

For each participant, trial-wise autocorrelation coefficients were estimated using the R-function *acf* with a maximum lag defined by the number of trials available per subject. Autocorrelation coefficients are displayed against the lag (in numbers of trials, ranging from 1 to 20) relative to the index trial (t = 0, see Figure 2B-C, 3B-C and 4B-C). To account for spurious autocorrelations that occur due to imbalances in the analyzed variables, we

estimated autocorrelations for randomly permuted data (100 iterations). For group-level autocorrelations, we computed the differences between the true autocorrelation coefficients and the mean autocorrelation observed for randomly permuted data and averaged across participants.

At a given trial, group-level autocorrelation coefficients were considered significant when linear mixed effects modeling indicated that the difference between real and permuted autocorelation coefficients was above zero at an alpha level of 0.05%. To test whether the autocorrelation of stimulus- and history-congruence remained significant when controlling for task difficulty and the sequence of presented stimuli, we added the respective autocorrelation as an additional factor to the linear mixed effects model that computed the group-level statistics (see also *Mixed effects modeling*).

To assess autocorrelations at the level of individual participants, we counted the number of subsequent trials (starting at the first trial after the index trial) for which less than 50% of the permuted autocorrelation coefficients exceeded the true autocorrelation coefficient. For example, a count of zero indicates that the true autocorrelation coefficients exceeded *less than 50%* of the autocorrelation coefficients computed for randomly permuted data at the first trial following the index trial. A count of five indicates that, for the first five trials following the index trial, the true autoccorrelation coefficients exceeded *more than 50%* of the respective autocorrelation coefficients for the randomly permuted data; at the sixt trial following the index trial, however, *less than 50%* of the autocorrelation coefficients exceeded the respective permuted autocorrelation coefficients.

6.3.4 Spectral densities

We used the R function *spectrum* to compute the spectral densities for the dynamic probabilities of stimulus- and history-congruence as well as the phase and coherence between the two variables. Periodograms were smoothed using modified Daniell smoothers at a width of 50. Since the dynamic probabilities of history- and stimulus-congruence were computed

using a sliding windows of ± 5 trials (i.e., intervals containing a total of 11 trials), spectral analyses were carried out for frequency below 1/11 $1/N_{trials}$. Please note that, throughout this manuscript, frequency has the dimensions of cycles per trial $1/N_{trials}$ rather than cycles per second (Hz).

6.4 Quantification and statistical procedures

All aggregate data are reported and displayed with errorbars as mean $\pm$ standard error of the mean.

6.4.1 Mixed effects modeling

Unless indicated otherwise, we performed group-level inference using the R-packages *lmer* and *afex* for linear mixed effects modeling and *glmer* with a binomial link-function for logistic regression. We compared models based on Akaike Information Criteria (AIC). To account for variability between the studies available from the Confidence Database[19], mixed modeling was conducted using random intercepts defined for each study. To account for variability across experimental session within the IBL database[20], mixed modeling was conducted using random intercepts defined for each individual session. When multiple within-participant datapoints were analyzed, we estimated random intercepts for each participant that were *nested* within the respective study or session. We report β values refering to the estimate of mixed effects modeling, followed by the respective T statistic (linear models) or z statistic (logistic models).

The effects of stimulus- and history-congruence on RTs and confidence reports (Figure 2-4, subpanel G-I) were assessed in linear mixed effects models that tested for main effects of both stimulus- and history-congruence as well as the between-factor interaction. Thus, the significance of any effect of history-congruence on RTs and confidence reports was assessed while controlling for the respective effect of stimulus-congruence (and vice versa).

6.4.2 Computational modeling

Model definition: Our modeling analysis is an extension of a model proposed by Glaze et al.[51], who defined a normative account of evidence accumulation for decision-making. In this model, trial-wise choices are explained by applying Bayes theorem to infer moment-by-moment changes in the state of environment from trial-wise noisy observations across trials.

Following Glaze et al.[51], we applied Bayes rule to compute the posterior evidence for the two alternative choices (i.e., the log posterior ratio L) from the sensory evidence available at time-point t (i.e., the log likelihood ratio LLR) with the prior probability ψ:

$$L_t = LLR_t * \omega_{LLR} + \psi_t(L_{t-1}, H) * \omega_\psi \tag{3}$$

In the trial-wise design studied here, a transition between the two states of the environment (i.e., the sources generating the noisy observations available to the participant) can occur at any time. Despite the random nature of the psychophysical paradigms studied here[19,20], humans and mice showed significant biases toward preceding choices (Figure 2A and 3A). We thus assumed that the prior probability of the two possible outcomes depends on the posterior choice probability at the preceding trial and the hazard rate H assumed by the participant. Following Glaze et al.[51], the prior ψ is thus computed as follows:

$$\psi_t(L_{t-1}, H) = L_{t-1} + log(\frac{1-H}{H} + exp(-L_{t-1})) - log(\frac{1-H}{H} + exp(L_{t-1})) \tag{4}$$

In this model, humans, mice and simulated agents make perceptual decision based on noisy observations u. The are computed by applying a sensitivity parameter α to the content of external sensory information I. For humans, we defined the input I by the two alternative states of the environment (outcome A: 0; coutcome B: 1), which generated the the observations u through a sigmoid function that applied a sensitivity parameter α:

$$u_t = \frac{1}{1 + exp(-\alpha * (I_t - 0.5))} \tag{5}$$

In mice, the inputs I were defined by the respective stimulus contrast in the two hemifields:

$$I_t = Contrast_{Right} - Contrast_{Left} \tag{6}$$

As in humans, we derived the input u by applying a sigmoid function with a sensitivity parameter α to input I:

$$u_t = \frac{1}{1 + exp(-\alpha * I_t)} \tag{7}$$

For humans, mice and in simulations, the log likelihood ratio LLR was computed from u as follows:

$$LLR_t = log(\frac{u_t}{1 - u_t}) \tag{8}$$

To allow for long-range autoccorelation in stimulus- and history-congruence (Figure 2B and 3B), our modeling approach differed from Glaze et al.[51] in that it allows for systematic fluctuation in the impact of sensory information (i.e., LLR) and the prior probability of choices ψ on the posterior probability L. This was achieved by multiplying the log likelihood ratio and the log prior ratio with coherent anti-phase fluctuations according to $\omega_{LLR} = amp_{LLR} * sin(f * t + phase) + 1$ and $\omega_\psi = amp_\psi * sin(f * t + phase + \pi) + 1$.

Model fitting: In model fitting, we predicted the trial-wise choices y_t (option A: 0; option B: 1) from inputs I. To this end, we minimized the log loss between y_t and the choice probability $prob_t$ in the unit interval. $prob_t$ was derived from L_t using a sigmoid function defined by the inverse decision temperature ζ:

$$prob_t = \frac{1}{1 + exp(-\zeta * L_t)} \tag{9}$$

This allowed us to infer the free parameters H (lower bound = 0, upper bound = 1; human posterior = 0.45 ± 4.8×10^{-5}; murine posterior = 0.46 ± 2.97×10^{-4}), α (lower bound = 0, upper bound = 5; human posterior = 0.5 ± 1.12×10^{-4}; murine posterior = 1.06 ± 2.88×10^{-3}), amp_ψ (lower bound = 0, upper bound = 10; human posterior = 1.44 ± 5.27×10^{-4}; murine posterior = 1.71 ± 7.15×10^{-3}), amp_{LLR} (lower bound = 0, upper bound = 10; human posterior = 0.5 ± 2.02×10^{-4}; murine posterior = 0.39 ± 1.08×10^{-3}), frequency f (lower bound = 1/40, upper bound = 1/5; human posterior = 0.11 ± 1.68×10^{-5}; murine posterior = 0.11 ± 1.63×10^{-4}) and *phase* (lower bound = 0, upper bound = 2*π; human posterior = 2.72 ± 4.41×10^{-4}; murine posterior = 2.83 ± 3.95×10^{-3}).

To validate our model, we correlated individual posterior parameter estimates with the respective conventional variables. We assumed that, (i), the estimated hazard rate H should correlate negatively with the frequency of history-congruent choices and that, (ii), the estimated α should correlate positively with the frequency of stimulus-congruent choices. In addition, we tested whether the posterior decision certainty (i..e. the absolute of the posterior log ratio) correlated negatively with RTs and positively with subjective confidence. This allowed us to assess whether our model could explain aspects of the data it was not fitted to (i.e., RTs and confidence). Finally, we used simulations (see below) to show that all model components, including the anti-phase oscillations governed by amp_ψ, amp_{LLR}, f and *phase*, were necessary for our model to reproduce the empirical data observed for the Confidence database[19] and IBL database[20].

Model simulation: We used the posterior model parameters observed for humans (H, α, amp_ψ, amp_{LLR} and f) to define individual parameters for simulation in 4317 simulated participants (i.e., equivalent to the number of human participants). For each participant, the number of simulated choices was drawn from a uniform distribution ranging from 300 to 700

trials. Inputs I were drawn at random for each trial, such that the sequence of inputs to the simulation did not contain any systematic seriality. Noisy observations u were generated by applying the posterior parameter α to inputs I, thus generating stimulus-congruent choices in $71.36 \pm 2.6 \times 10^{-3}\%$ of trials. Choices were simulated based on the trial-wise choice probabilities y_{prob}. Simulated data were analyzed in analogy to the human and murine data. As a substitute of subjective confidence, we computed the absolute of the trial-wise posterior log ratios $|L|$ (i.e., the posterior decision certainty).

7 Figures

7.1 Figure 1

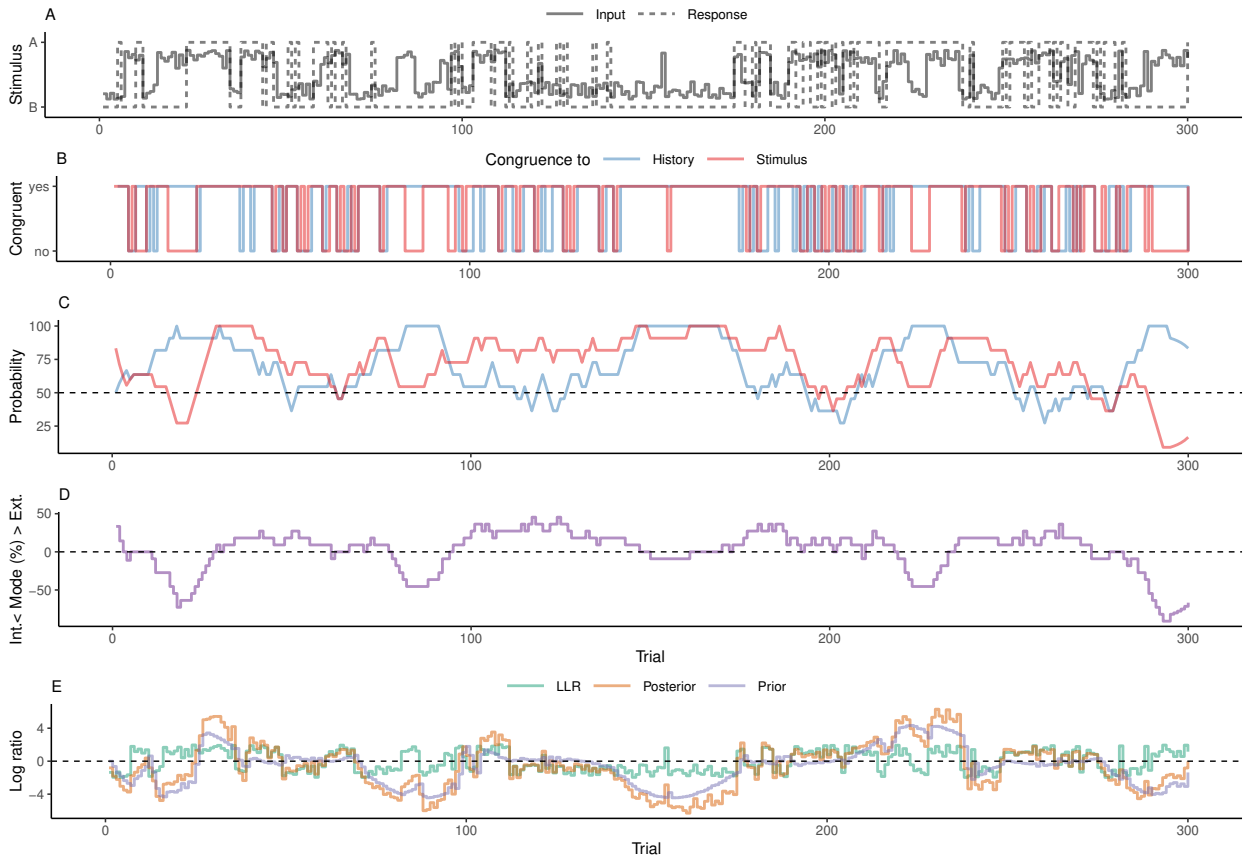

Figure 1. Concept.

A. In binary perceptual decision-making, a participant is presented with stimuli from two categories (A vs. B; dotted line) and reports consecutive perceptual choices via button presses (sold line). All panels below refer to this example data.

B. When the response matched the external stimulus information (i.e., overlap between dotted and solid line in panel A), perceptual choices are *stimulus-congruent* (red line). When the response matches the response at the preceding trial, perceptual choices are *history-congruent* (blue line).

C. The dynamic probabilities of stimulus- and history-congruence (i.e., computed in sliding windows of ±5 trials) fluctuate over time.

D. The *mode* of perceptual processing is derived by computing the difference between the dynamic probabilities of stimulus- and history-congruence. Values above 0% indicate a bias toward external information, whereas values below 0% indicate a bias toward internal information.

E. In computational modeling, internal mode is caused by an enhanced impact of perceptual history. This causes the posterior (orange line) to be close to the prior (purple). Conversely, during external mode, the posterior is close to the sensory information (log likelihood ratio, green line).

7.2 Figure 2

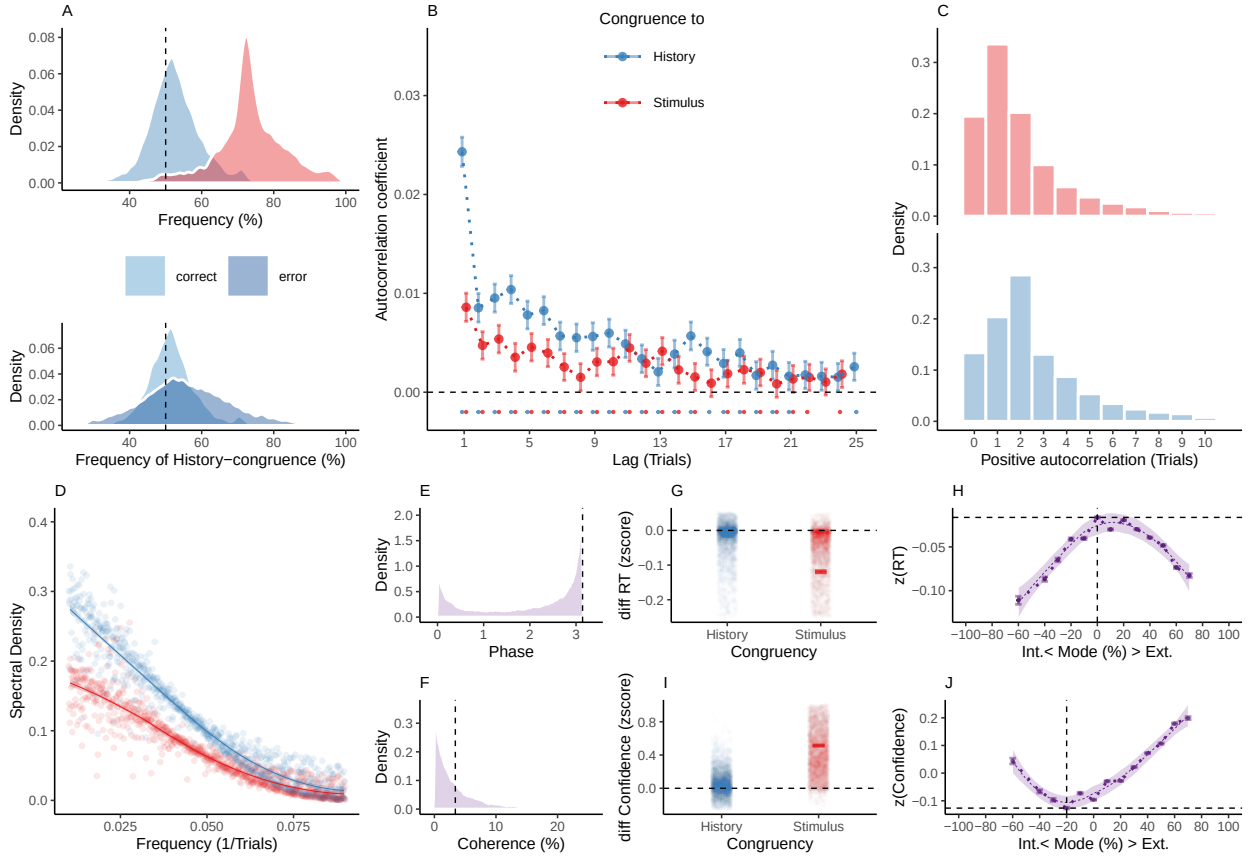

Figure 2. Internal and external modes in human perceptual decision-making.

A. In humans, perception was stimulus-congruent in 73.46% ± 0.15% (in red) and history-congruent in 52.89% ± 0.12% of trials (in blue; upper panel). History-congruent perceptual choices were more frequent when perception was stimulus-incongruent (i.e., on *error* trials; lower panel), indicating that history effects impair performance in randomized psychophysical designs.

B. Relative to randomly permuted data, we found highly significant autocorrelations of stimulus-congruence and history-congruence (dots indicate intercepts $\neq 0$ in trial-wise linear mixed effects modeling at $p < 0.05$). Across trials, the autocorrelation coefficients were best fit by an exponential function (adjusted R^2 for stimulus-congruence: 0.57; history-congruence: 0.72) as compared to a linear function (adjusted R^2 for stimulus-congruence:

0.56; history-congruence: 0.51).

C. Here, we depict the number of consecutive trials at which autocorrelation coefficients exceeded the respective autocorrelation of randomly permuted data within individual participants. For stimulus-congruence (upper panel), the lag of positive autocorrelation amounted to $3.24 \pm 2.39 \times 10^{-3}$ on average, showing a peak at trial t+1 after the index trial. For history-congruence (lower panel), the lag of positive autocorrelation amounted to $4.87 \pm 3.36 \times 10^{-3}$ on average, peaking at trial t+2 after the index trial.

D. The smoothed probabilities of stimulus- and history-congruence (sliding windows of ± 5 trials) oscillated as *1/f noise*, i.e., at power densities that were inversely proportional to the frequency.

E. The distribution of phase shift between fluctuations in stimulus- and history-congruence peaked at half a cycle (π denoted by dotted line).

F. The average coherence between fluctuations in stimulus- and history-congruence (black dottet line) amounted to $6.49 \pm 2.07 \times 10^{-3}\%$

G. We observed faster response times (RTs) for both stimulus-congruence (as opposed to stimulus-incongruence, $\beta = -0.14 \pm 1.61 \times 10^{-3}$, $\mathrm{T}(1.99 \times 10^{6}) = -85.93$, $\mathrm{p} < 2.2 \times 10^{-308}$) and history-congruence ($\beta = -9.68 \times 10^{-3} \pm 1.38 \times 10^{-3}$, $\mathrm{T}(1.99 \times 10^{6}) = -7.02$, $\mathrm{p} = 2.16 \times 10^{-12}$).

H. The mode of perceptual processing (i.e., the difference between the smoothed probability of stimulus- vs. history-congruence) showed a quadratic relationship to RTs, with faster response times for stronger biases toward both external sensory information and internal predictions provided by perceptual history ($\beta_2 = -19.86 \pm 0.52$, $\mathrm{T}(1.98 \times 10^{6}) = -38.43$, $\mathrm{p} = 5 \times 10^{-323}$). The horizontal and vertical dotted lines indicate maximum RT and the associated mode, respectively.

I. Confidence was enhanced for both stimulus-congruence (as opposed to stimulus-

incongruence, $\beta = 0.49 \pm 1.38 \times 10^{-3}$, $\mathrm{T}(2.06 \times 10^6) = 352.16$, $\mathrm{p} < 2.2 \times 10^{-308}$) and history-congruence ($\beta = 0.04 \pm 1.18 \times 10^{-3}$, $\mathrm{T}(2.06 \times 10^6) = 36.71$, $\mathrm{p} = 7.5 \times 10^{-295}$).

J. In analogy to RTs, we found a quadratic relationship between the mode of perceptual processing and confidence, which increased when both externally- and internally-biased modes grew stronger ($\beta_2 = 39.3 \pm 0.94$, $\mathrm{T}(2.06 \times 10^6) = 41.95$, $\mathrm{p} < 2.2 \times 10^{-308}$). The horizontal and vertical dotted lines indicate mimimum confidence and the associated mode, respectively.

7.3 Figure 3

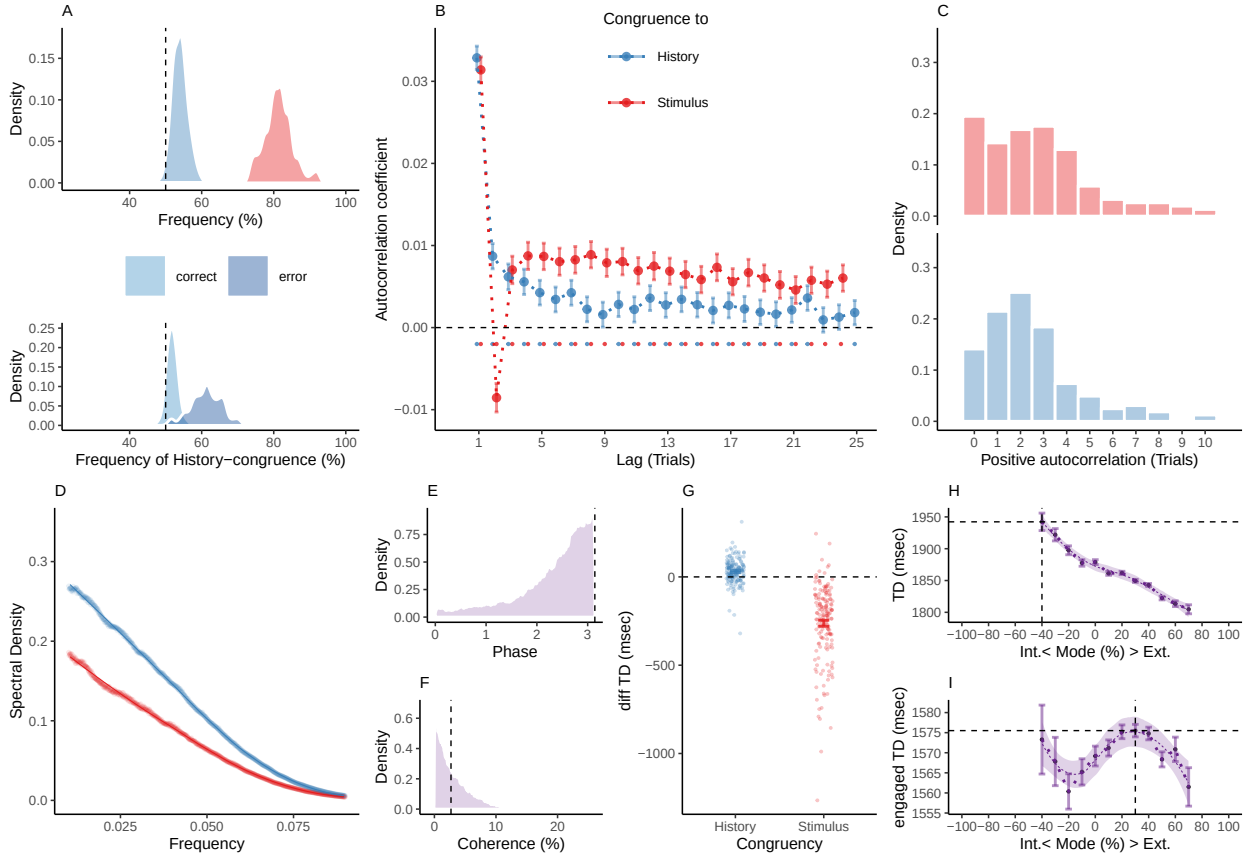

Figure 3. Internal and external modes in murine perceptual decision-making.

A. In mice, 81.37% ± 0.3% of trials were stimulus-congruent (in red) and 54.03% ± 0.17% of trials were history-congruent (in blue; upper panel). History-congruent perceptual choices were not a consequence of the experimental design, but a source of error, as they were more frequent on stimulus-incongruent trials (lower panel).

B. Relative to randomly permuted data, we found highly significant autocorrelations of stimulus-congruence and history-congruence (dots indicate intercepts $\neq 0$ in trial-wise linear mixed effects modeling at $p < 0.05$). Please note that the negative autocorrelation of stimulus-congruence at trial 2 was a consequence of the experimental desgin (see Supplemental Figure 2D-F). As in humans, autocorrelation coefficients were best fit by an exponential function (adjusted R^2 for stimulus-congruence: 0.44; history-congruence: 0.52) as compared to a linear

function (adjusted R^2 for stimulus-congruence: 3.16×10^{-3}; history-congruence: 0.26).

C. For stimulus-congruence (upper panel), the lag of positive autocorrelation was longer in comparison to humans (4.59 ± 0.06 on average). For history-congruence (lower panel), the lag of positive autocorrelation was sligthly shorter relative to humans (2.58 ± 0.01 on average, peaking at trial t+2 after the index trial).

D. In mice, the dynamic probabilities of stimulus- and history-congruence (sliding windows of ± 5 trials) fluctuated as *1/f noise*.

E. The distribution of phase shift between fluctuations in stimulus- and history-congruence peaked at half a cycle (π denoted by dotted line).

F. The average coherence between fluctuations in stimulus- and history-congruence (black dottet line) amounted to $3.45 \pm 0.01\%$

G. We observed shorter trial durations (TDs) for stimulus-congruence (as opposed to stimulus-incongruence, $\beta = -1.12 \pm 8.53 \times 10^{-3}$, $\mathrm{T}(1.34 \times 10^6) = -131.78$, $\mathrm{p} < 2.2 \times 10^{-308}$), but longer TDs for history-congruence ($\beta = 0.06 \pm 6.76 \times 10^{-3}$, $\mathrm{T}(1.34 \times 10^6) = 8.52$, $\mathrm{p} = 1.58 \times 10^{-17}$).

H. TDs decreased monotonically for stronger biases toward external mode ($\beta_1 = -4.36 \times 10^4 \pm 1.27 \times 10^3$, $\mathrm{T}(1.24 \times 10^6) = -34.31$, $\mathrm{p} = 8.43 \times 10^{-258}$). The horizontal and vertical dotted lines indicate maximum TD and the associated mode, respectively.

I. For TDs that differed from the median TD by no more than 1.5 x MAD (median absolute distance[49]), mice exhibited a quadratic component in the relationship between the mode of sensory processing and TDs ($\beta_2 = -2.02 \times 10^3 \pm 835.64$, $\mathrm{T}(1.1 \times 10^6) = -2.42$, $\mathrm{p} = 0.02$, Figure 3I). This explorative post-hoc analysis focuses on trials at which mice engage more swiftly with the experimental task. The horizontal and vertical dotted lines indicate maximum TD and the associated mode, respectively.

7.4 Figure 4

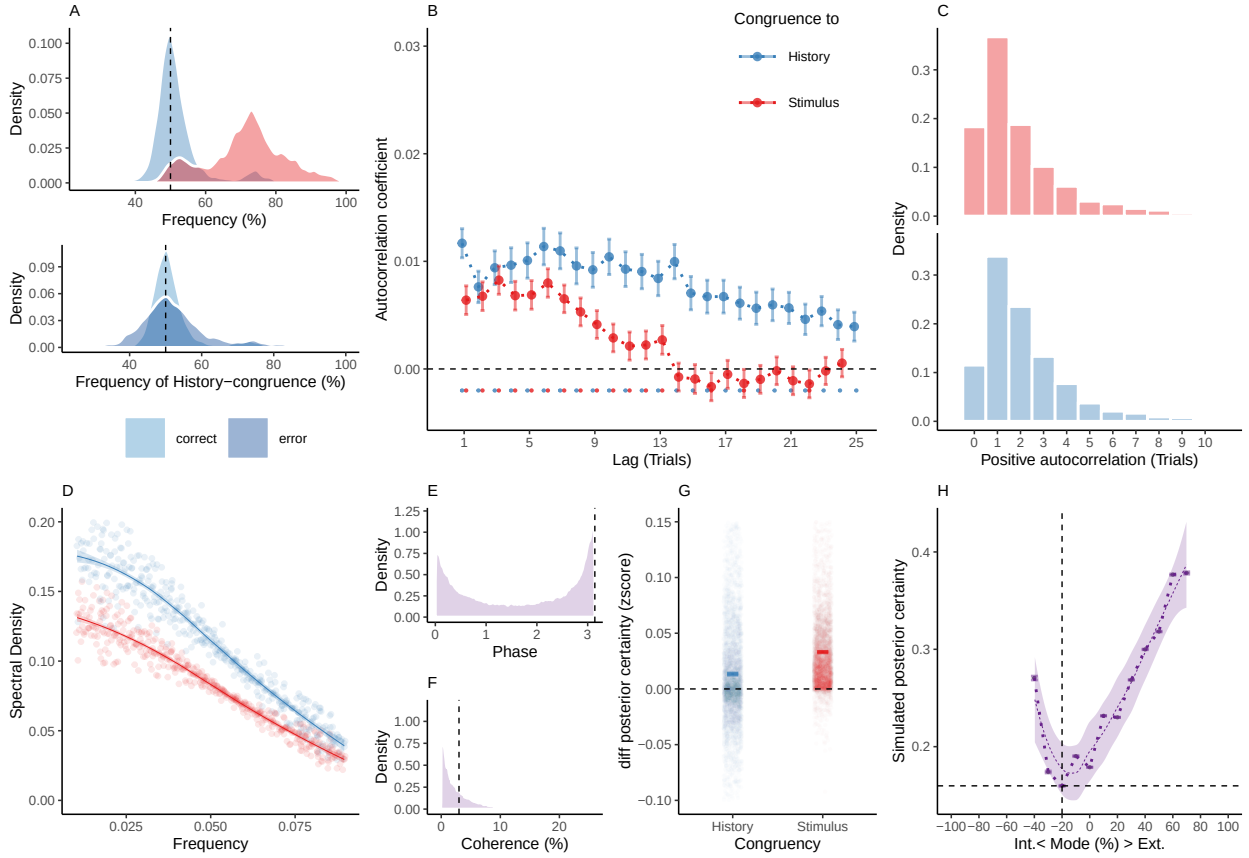

Figure 4. Internal and external modes in simulated perceptual decision-making.

A. Simulated perceptual choices were stimulus-congruent in 71.36% ± 0.17% (in red) and history-congruent in 51.99% ± 0.11% of trials (in blue; $T(4.32 \times 10^3) = 17.42$, $p = 9.89 \times 10^{-66}$; upper panel). Due to the competition between stimulus- and history-congruence, history-congruent perceptual choices were more frequent when perception was stimulus-incongruent (i.e., on *error* trials; $T(4.32 \times 10^3) = 11.19$, $p = 1.17 \times 10^{-28}$; lower panel) and thus impaired performance in the randomized psychophysical design simulated here.

B. At the simulated group level, we found significant autocorrelations in both stimulus-congruence (13 consecutive trials) and history-congruence (30 consecutive trials).

C. On the level of individual simulated participants, autocorrelation coefficients exceeded the autocorrelation coefficients of randomly permuted data within a lag of $2.46 \pm 1.17 \times 10^{-3}$

trials for stimulus-congruence and $4.24 \pm 1.85 \times 10^{-3}$ trials for history-congruence.

D. The smoothed probabilities of stimulus- and history-congruence (sliding windows of ± 5 trials) oscillated as *1/f noise*, i.e., at power densities that were inversely proportional to the frequency (power $\sim 1/f^{\beta}$; stimulus-congruence: $\beta = -0.81 \pm 1.18 \times 10^{-3}$, $\mathrm{T}(1.92 \times 10^{5}) = -687.58$, $\mathrm{p} < 2.2 \times 10^{-308}$; history-congruence: $\beta = -0.83 \pm 1.27 \times 10^{-3}$, $\mathrm{T}(1.92 \times 10^{5}) = -652.11$, $\mathrm{p} < 2.2 \times 10^{-308}$).

E. The distribution of phase shift between fluctuations in simulated stimulus- and history-congruence peaked at half a cycle (π denoted by dotted line). The dynamic probabilities of simulated stimulus- and history-congruence were therefore were strongly anti-correlated ($\beta = -0.03 \pm 8.22 \times 10^{-4}$, $\mathrm{T}(2.12 \times 10^{6}) = -40.52$, $\mathrm{p} < 2.2 \times 10^{-308}$).

F. The average coherence between fluctuations in simulated stimulus- and history-congruence (black dottet line) amounted to $6.49 \pm 2.07 \times 10^{-3}\%$.

G. Simulated confidence was enhanced for stimulus-congruence ($\beta = 0.03 \pm 1.71 \times 10^{-4}$, $\mathrm{T}(2.03 \times 10^{6}) = 178.39$, $\mathrm{p} < 2.2 \times 10^{-308}$) and history-congruence ($\beta = 0.01 \pm 1.5 \times 10^{-4}$, $\mathrm{T}(2.03 \times 10^{6}) = 74.18$, $\mathrm{p} < 2.2 \times 10^{-308}$).

H. In analogy to humans, the simulated data showed a quadratic relationship between the mode of perceptual processing and posterior certainty, which increased for stronger external and internal biases ($\beta_2 = 31.03 \pm 0.15$, $\mathrm{T}(2.04 \times 10^{6}) = 205.95$, $\mathrm{p} < 2.2 \times 10^{-308}$). The horizontal and vertical dotted lines indicate mimimum posterior certainty and the associated mode, respectively.

8 Supplemental Items

8.1 Supplemental Figure S1

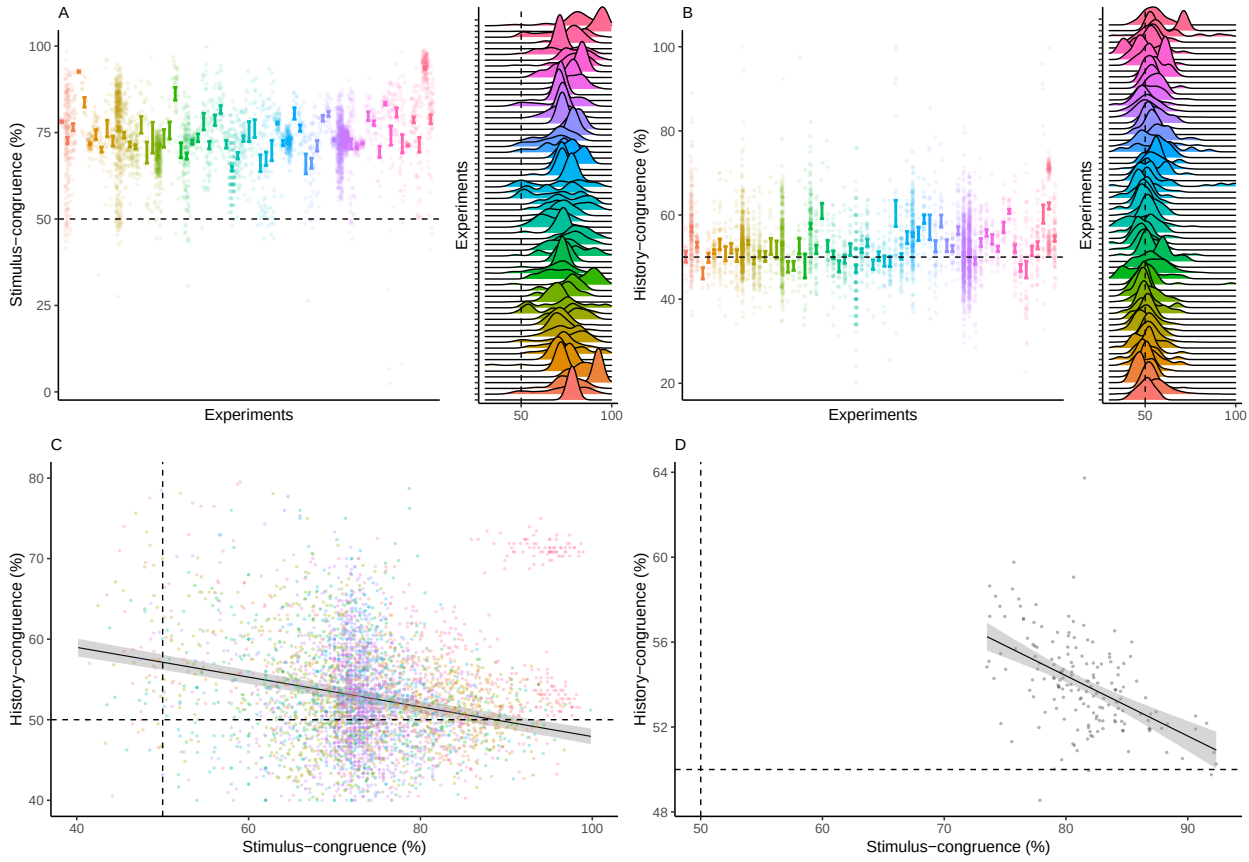

Supplemental Figure S1. Stimulus- and history-congruence.

A. Stimulus-congruent choices in humans amounted to 73.46% ± 0.15% of trials and were highly consistent across the experiments selected from the Confidence Database.

B. History-congruent choices in humans amounted to 52.89% ± 0.12% of trials. In analogy to stimulus-congruence, the prevalence of history-congruence was highly consistent across the experiments selected from the Confidence Database. 50% of experiments showed significant ($p < 0.05$) attractive biases toward preceding choices, whereas 3.03% of experiments showed significant repulsive biases.

C. In humans, we found an enhanced impact of perceptual history in participants who were

less sensitive to external sensory information (T(4.3×10^3) = -14.32, p = 1.72×10^{-45}), suggesting that perception results from the competition of external with internal information.

D. In analogy to humans, mice that were less sensitive to external sensory information showed stronger biases toward perceptual history (T(163) = -7.52, p = 3.44×10^{-12}, Pearson correlation).

8.2 Supplemental Figure S2

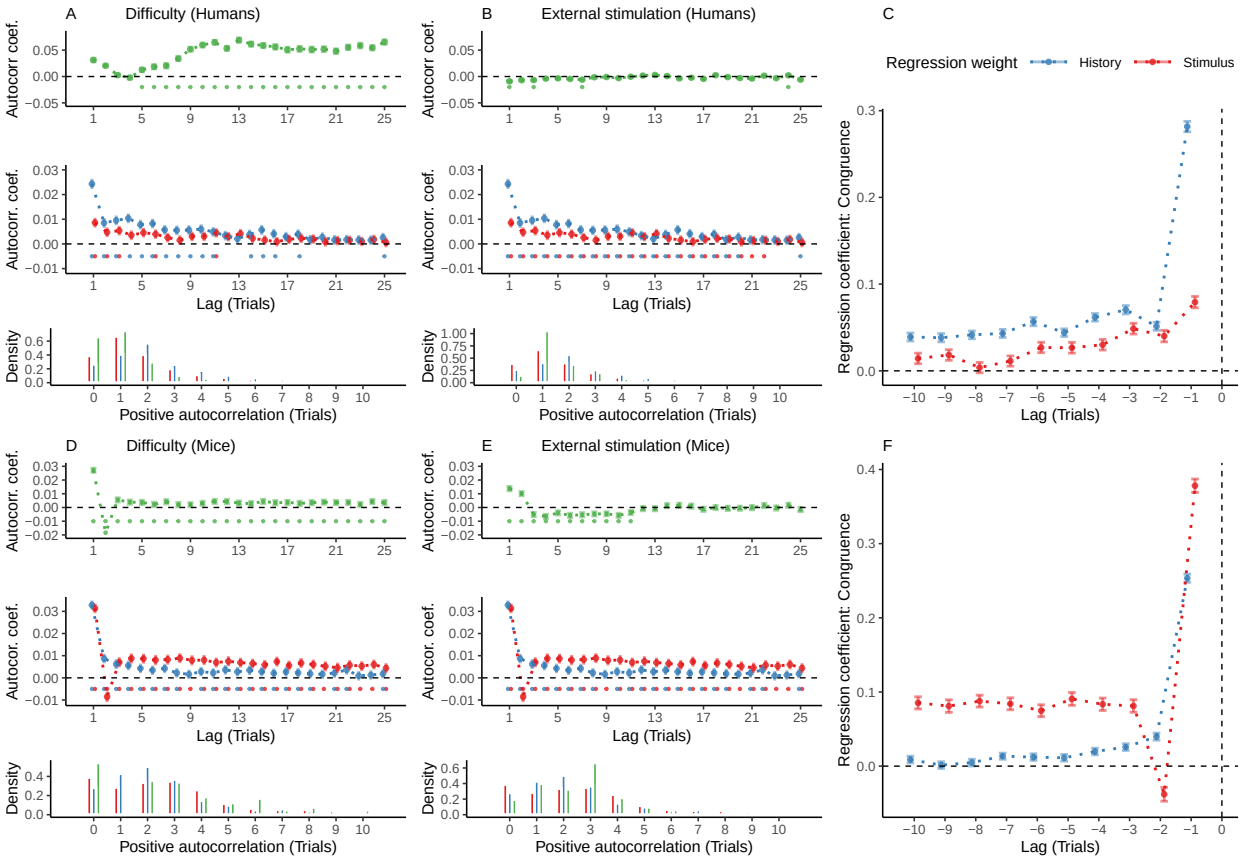

Supplemental Figure S2. Controlling for task difficulty and external stimulation. In this study, we found highly significant autocorrelations of stimulus- and history-congruence in humans as well as in mice. Here, we show that these autocorrelations are not a trivial consequence of task difficulty or the sequence external stimulation. In addition, we computed trial-wise logistic regression coefficients as an alternative approach to assessing serial dependencies in stimulus- and history-congruence.

A. In humans, task difficulty (in green) showed a significant autocorrelated starting at the 5th trial (upper panel, dots at the bottom indicate intercepts $\neq 0$ in trial-wise linear mixed effects modeling at $p < 0.05$). When controlling for task difficulty, linear mixed effects modeling indicated a significant auto-correlation of stimulus-congruence (in red) for the first 3 consecutive trials (middle panel). 20% of trials within the displayed time window remained significantly autocorrelated. The autocorrelation of history-congruence (in blue) remained

significant for the first 11 consecutive trials (64% significantly autocorrelated trials within the displayed time window). At the level of individual participants, the autocorrelation of task difficulty exceeded the respective autocorrelation of randomly permuted within a lag of $21.66 \pm 8.37 \times 10^{-3}$ trials (lower panel).

B. The sequence of external stimulation (i.e., which of the two binary outcomes was supported by the presented stimuli; depicted in green) was negatively autocorrelated for 1 trial. When controlling for the autocorrelation of external stimulation, stimulus-congruence remained significantly autocorrelated for 22 consecutive trials (88% of trials within the displayed time window; lower panel) and history-congruence remained significantly autocorrelated for 20 consecutive trials (84% of trials within the displayed time window). At the level of individual participants, the autocorrelation of external stimulation exceeded the respective autocorrelation of randomly permuted within a lag of $2.94 \pm 4.4 \times 10^{-3}$ consecutive trials (lower panel).

C. As an alternative to group-level autocorrelation coefficients, we used trial-wise logistic regression to quantify serial dependencies in stimulus- and history-congruence. This analysis predicted stimulus- and history-congruence at the index trial (trial $t = 0$, vertical line) based on stimulus- and history-congruence at the 10 preceding trials. Mirroring the shape of the group-level autocorrelations, trial-wise regression coefficients increased exponentially toward the index trial.

D. In mice, task difficulty showed an significant autocorrelated for the first 25 consecutive trials (upper panel). When controlling for task difficulty, linear mixed effects modeling indicated a significant auto-correlation of stimulus-congruence for the first 36 consecutive trials (middle panel). In total, 100% of trials within the displayed time window remained significantly autocorrelated. The autocorrelation of history-congruence remained significant for the first 8 consecutive trials, with 84% significantly autocorrelated trials within the displayed time window. At the level of individual mice, autocorrelation coefficients for difficulty were elevated

above randomly permuted data within a lag of 15.13 ± 0.19 consecutive trials (lower panel).

E. In mice, the sequence of external stimulation (i.e., which of the two binary outcomes was supported by the presented stimuli) was negatively autocorrelated for 11 consecutive trials (upper panel). When controlling for the autocorrelation of external stimulation, stimulus-congruence remained significantly autocorrelated for 86 consecutive trials (100% of trials within the displayed time window; middle) and history-congruence remained significantly autocorrelated for 8 consecutive trials (84% of trials within the displayed time window). At the level of individual mice, autocorrelation coefficients for external stimulation were elevated above randomly permuted data within a lag of $2.53 \pm 9.8 \times 10^{-3}$ consecutive trials (lower panel).

F. Following our results in human data, regression coefficients that predicted history-congruence at the index trial (trial t = 0, vertical line) increased exponentially for trials closer to the index trial. In contrast to history-congruence, stimulus-congruence showed a negative regression weight (or autocorrelation coefficient, see Figure 3B) at trial -2. This was due to the experimental design (see also the autocorrelations of difficulty and external stimulation in Supplemental Figure S2C and D): When mice made aerrors on easy trials (contrast $\geq$ 50%), the upcoming stimulus was shown at the same spatial location and at high contrast. This increased the probability of stimulus-congruent perceptual choices after stimulus-incongruent perceptual choices at easy trials, thereby creating a negative regression weight (or autocorrelation coefficient) of stimulus-congruence at trial -2.

8.3 Supplemental Figure S3

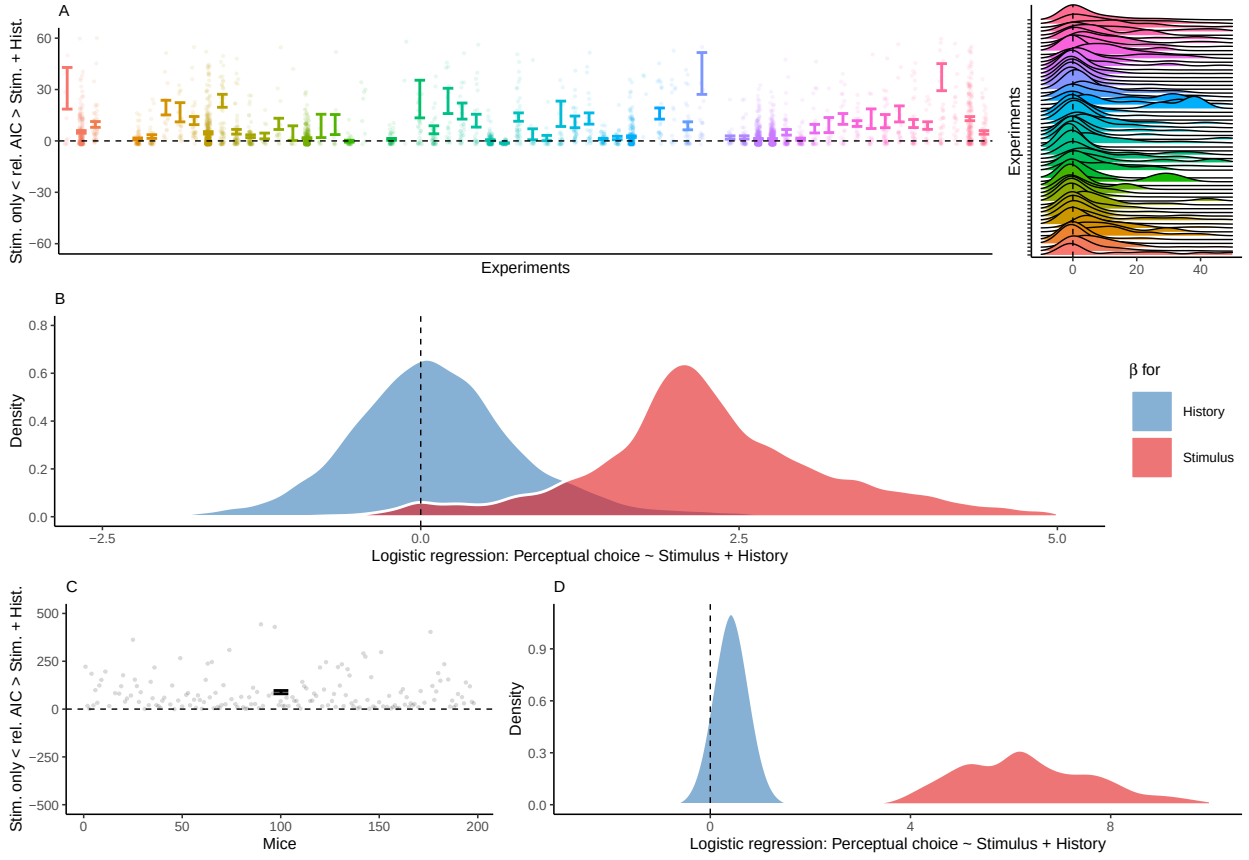

Supplemental Figure S3. Logistic regression A. To ensure that perceptual history played a significant role in perception despite the ongoing stream of external information, we tested whether human perceptual decision-making was better explained by the combination of external and internal information or, alternatively, by external information alone. To this end, we compared Aikake information criteria between logistic regression models that predicted trial-wise perceptual responses either by both current external sensory information and the preceding percept, or by external sensory information alone (values above zero indicate a superiority of the full model). With high consistency across the experiments selected from the Confidence Database, this model-comparison confirmed that perceptual history contributed significantly to perception (difference in AIC = 8.07 ± 0.53, $T(57.22) = 4.1$, $p = 1.31 \times 10^{-4}$).

B. Participant-wise regression coefficients amount to 0.18 ± 0.02 for the effect of perceptual history and 2.51 ± 0.03 for external sensory stimulation.

C. In mice, an AIC-based model comparison indicated that perception was better explained by logistic regression models that predicted trial-wise perceptual responses based on both current external sensory information and the preceding percept (difference in AIC = 88.62 $\pm$ 8.57, T(164) = 10.34, p = 1.29×10^{-19}).

D. In mice, individual regression coefficients amounted to 0.42 $\pm$ 0.02 for the effect of perceptual history and 6.91 $\pm$ 0.21 for external sensory stimulation.

8.4 Supplemental Figure S4

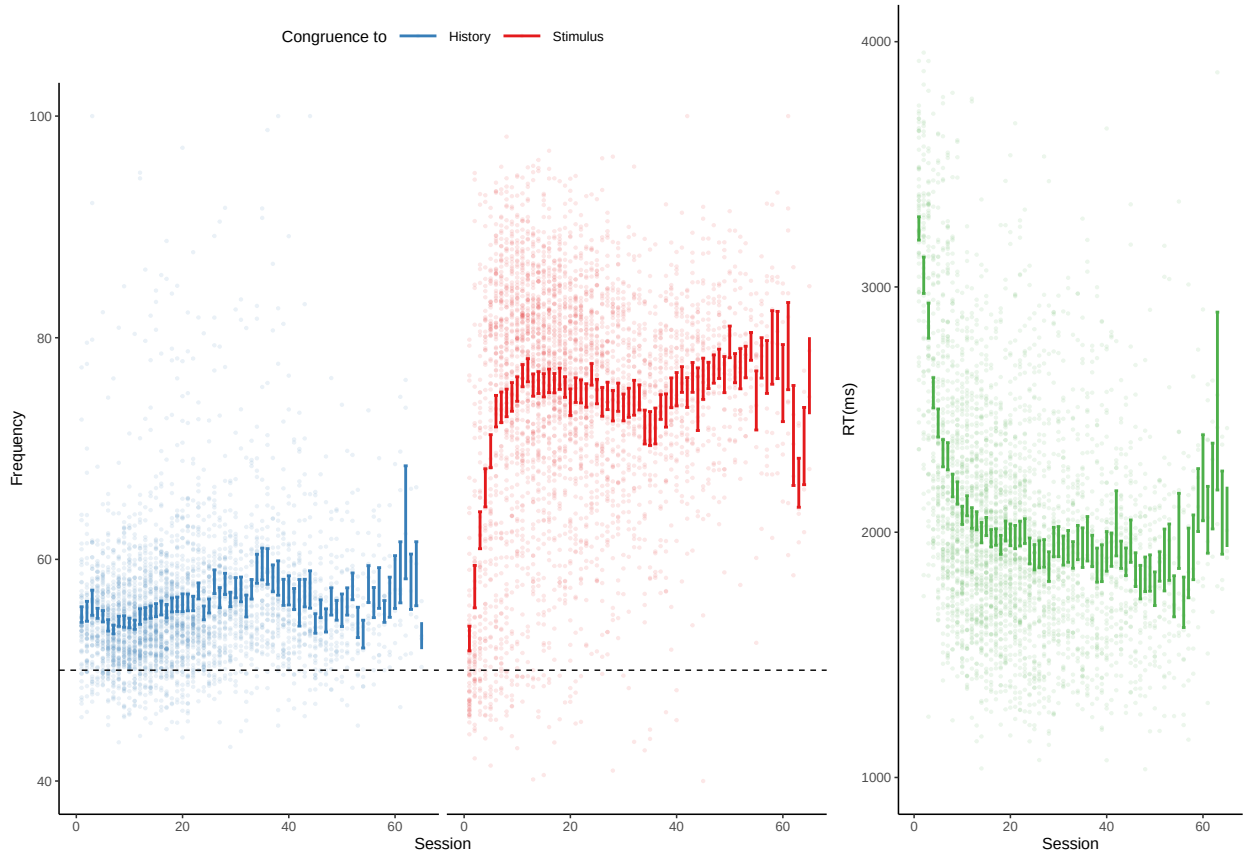

Supplemental Figure S4. History-/stimulus-congruence and TDs during training of the basic task.

Here, we depict the progression of history- and stimulus-congruence (depicted in blue and red, respectively; left panel) as well as TDs (in green; right panel) across training sessions in mice that achieved proficiency (i.e., stimulus-congruence $\geq 80\%$) in the *basic* task of the IBL dataset. We found that both history-congruent perceptual choices ($\beta = 0.13 \pm 4.67 \times 10^{-3}$, $\mathrm{T}(8.4 \times 10^3) = 27.04$, $\mathrm{p} = 1.96 \times 10^{-154}$) and stimulus-congruent perceptual choices ($\beta = 0.34 \pm 7.13 \times 10^{-3}$, $\mathrm{T}(8.51 \times 10^3) = 47.66$, $\mathrm{p} < 2.2 \times 10^{-308}$) became more frequent with training. As in humans, mice showed shorter TDs with increas exposure to the task ($\beta = -22.14 \pm 17.06$, $\mathrm{T}(1.14 \times 10^3) = -1.3$, $\mathrm{p} < 2.2 \times 10^{-308}$).

8.5 Supplemental Figure S5

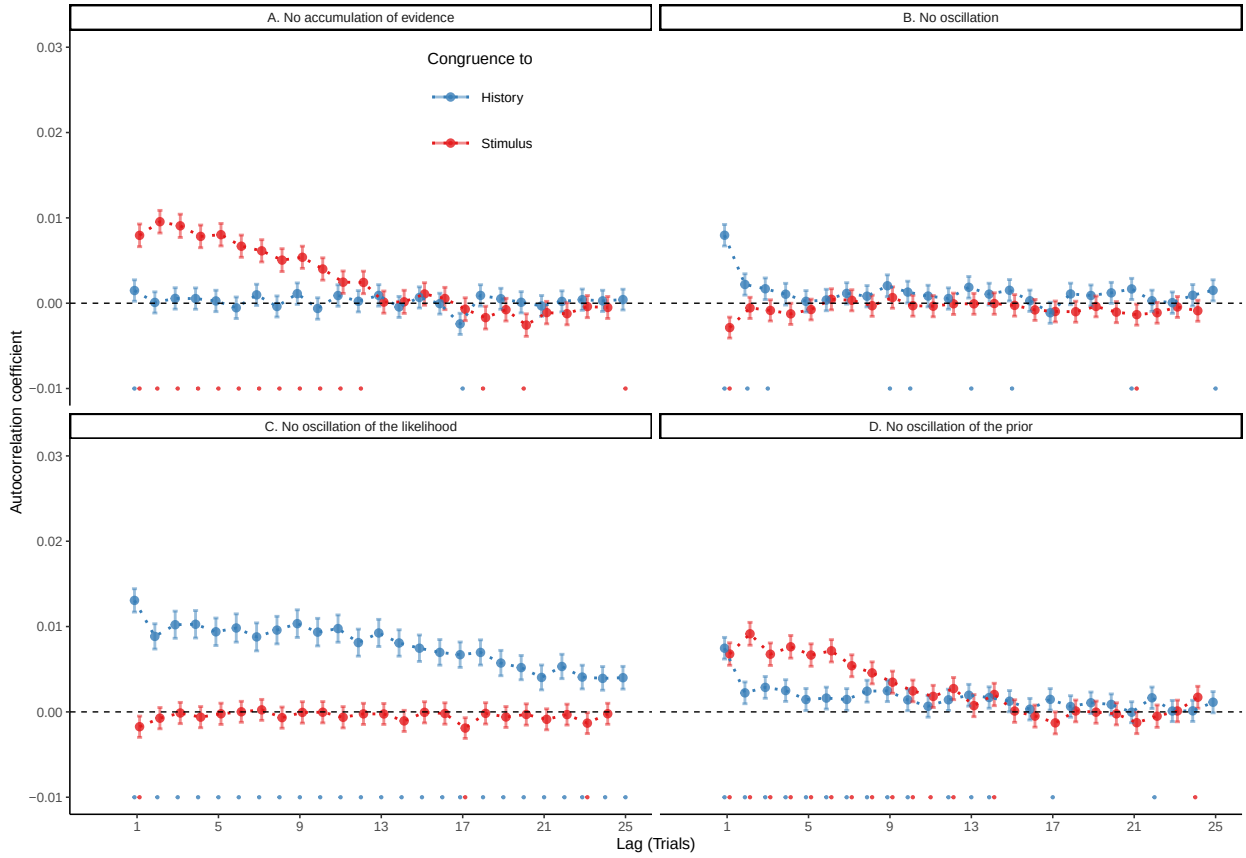

Supplemental Figure S5. Control Simulation: Reduced models. Here, we show group-level autocorrelations for reduced models. The dots at the bottom indicate a significant difference to randomly permuted data (intercept $\neq 0$ at $p < 0.05$).

A. When removing the accumulation of information across trials from the model (i.e., by settings the Hazard rate H to 0.5), we did not observe a significant autocorrelation of history-congruence beyond the first trial, whereas the autocorrelation of stimulus-congruence was preserved.

B. When removing all slow oscillations from the model (i.e., by setting both amp_{LLR} and amp_{ψ} to zero), we did not find significant autocorrelations for stimulus-congruence. Likewise, we did not observe any autocorrelation of history-congruence beyond the first three consecutive trials.

C. When removing the slow oscillation only from the likelihood term (i.e., by setting $amp_{LLR} = 0$), we did not observe any significant autocorrelation of stimulus-congruence beyond the first time, whereas the autocorrelation of history-congruence was preserved.

D. When removing the slow oscillation only from the prior term (i.e., by setting $amp_{psi} = 0$), we obeserved that the autocorrelation coefficients for history-congruence were reduced below the autocorrelation coefficients of stimulus-congruence. This is an approximately five-fold reduction relative to the empirical results observed in humans (Figure 2B), where the autocorrelation of history-congruence was above the autocorrelation of stimulus-congruence. Moreover, in the reduced model shown here, the number of consecutive trials that showed significant autocorrelation of history-congruence was reduced to 11 (empirical data in humans: significant autocorrelation for 21 consecutive trials).

8.6 Supplemental Figure S6

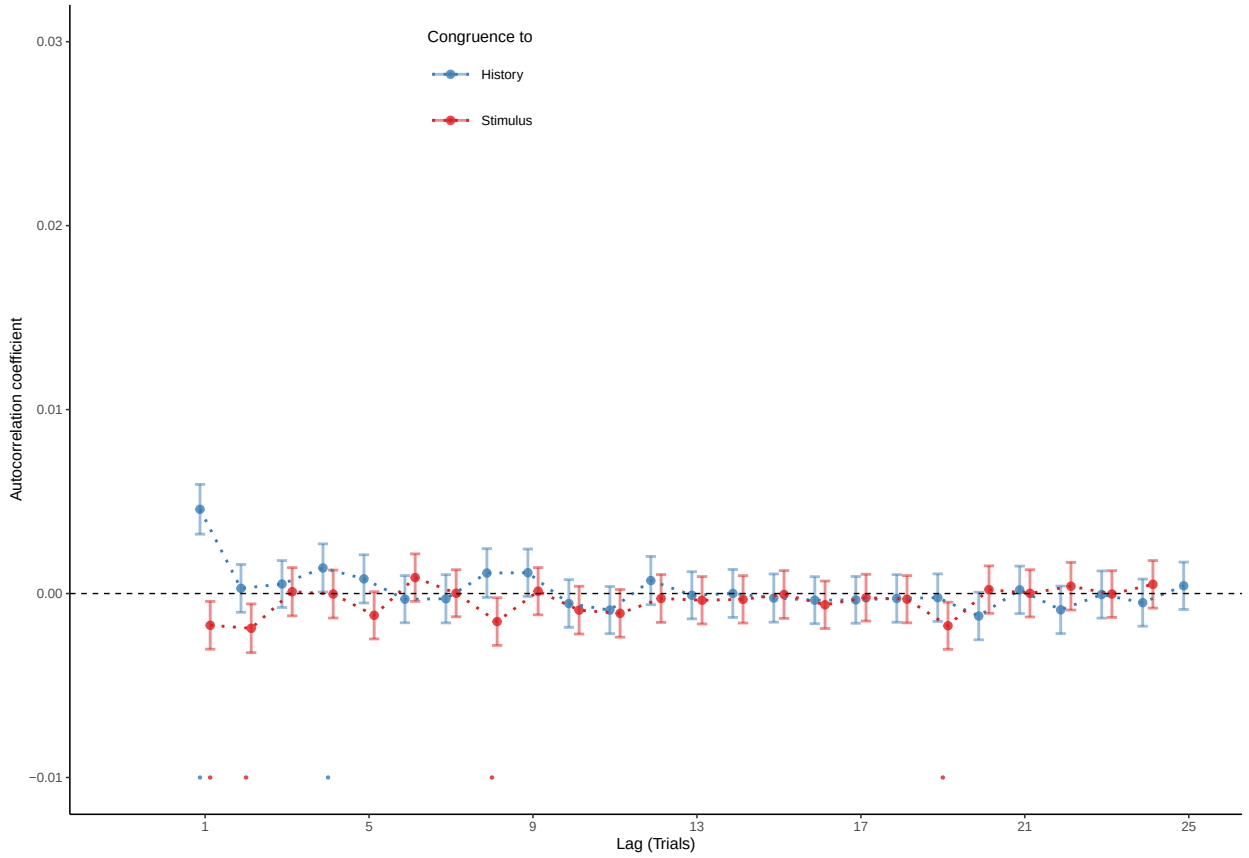

Supplemental Figure S6. Reset-Rebounce. Here, we show group-level autocorrelations for a reset-rebound-model[52] which assumes that errors cause perception to switch between two regimes: After an error, internal predictions became irrelavent for perceptual decision-making (*reset*: H = 0.5) until the agent makes a correct decision. After that, the agent restarts to accumulate sensory information across sucessive trials (*rebounce*: H $\neq$ 0.5), until the next errors occurs. Simulation based on this model did not reproduce any significant autocorrelation of stimulus- or history-congruence beyond the second or first trial, respectively.

8.7 Supplemental Table T1

Authors	Journal	Year
Bang, Shekhar, Rahnev	JEP:General	2019
Bang, Shekhar, Rahnev	JEP:General	2019
Calder-Travis, Charles, Bogacz, Yeung	Unpublished	NA
Clark & Merfeld	Journal of Neurophysiology	2018
Clark	Unpublished	NA
Faivre, Filevich, Solovey, Kuhn, Blanke	Journal of Neuroscience	2018
Faivre, Vuillaume, Blanke, Cleeremans	bioRxiv	2018
Filevich & Fandakova	Unplublished	NA
Gajdos, Fleming, Saez Garcia, Weindel, Davranche	Neuroscience of Consciousness	2019
Gherman & Philiastides	eLife	2018
Haddara & Rahnev	PsyArXiv	2020
Haddara & Rahnev	PsyArXiv	2020
Hainguerlot, Vergnaud, & de Gardelle	Scientific Reports	2018
Hainguerlot, Gajdos, Vergnaud, & de Gardelle	Unpublished	NA
Jachs, Blanco, Grantham-Hill, Soto	JEP:HPP	2015
Jachs, Blanco, Grantham-Hill, Soto	JEP:HPP	2015
Jachs, Blanco, Grantham-Hill, Soto	JEP:HPP	2015
Jaquiery, Yeung	Unpublished	NA
Kvam, Pleskac, Yu, Busemeyer	PNAS	2015
Kvam, Pleskac, Yu, Busemeyer	PNAS	2015
Kvam and Pleskac	Cognition	2016
Law, Lee	Unpublished	NA
Lebreton, et al.	Sci. Advances	2018
Lempert, Chen, & Fleming	PlosOne	2015
Locke*, Gaffin-Cahn*, Hosseinizaveh, Mamassian, & Landy	Attention, Perception, & Psychophysics	2020
Maniscalco, McCurdy,Odegaard, & Lau	J Neurosci	2017
Maniscalco, McCurdy,Odegaard, & Lau	J Neurosci	2017
Maniscalco, McCurdy,Odegaard, & Lau	J Neurosci	2017
Maniscalco, McCurdy,Odegaard, & Lau	J Neurosci	2017
Martin, Hsu	Unpublished	NA
Massoni & Roux	Journal of Mathematical Psychology	2017
Massoni	Unpublished	NA
Mazor, Friston & Fleming	eLife	2020
Mei, Rankine,Olafsson, Soto	bioRxiv	2019
Mei, Rankine,Olafsson, Soto	bioRxiv	2019
O'Hora, Zgonnikov, Kenny, Wong-Lin	Fechner Day proceedings	2017
O'Hora, Zgonnikov, CiChocki	Unpublished	NA

(continued)

Authors	Journal	Year
O'Hora, Zgonnikov, Neverauskaite	Unpublished	NA
Palser et al	Consciousness & Cognition	2018
Pereira, Faivre, Iturrate et al.	bioRxiv	2018
Prieto et al.	Submitted	NA
Rahnev et al	J Neurophysiol	2013
Rausch & Zehetleitner	Front Psychol	2016
Rausch et al	Attention, Perception, & Psychophysics	2018
Rausch et al	Attention, Perception, & Psychophysics	2018
Rausch, Zehetleitner, Steinhauser, & Maier	NeuroImage	2020
Recht, de Gardelle & Mamassian	Unpublished	NA
Reyes et al.	PlosOne	2015
Reyes et al.	Submitted	NA
Rouault, Seow, Gillan, Fleming	Biol. Psychiatry	2018
Rouault, Seow, Gillan, Fleming	Biol. Psychiatry	2018
Rouault, Dayan, Fleming	Nat Commun	2019
Sadeghi et al	Scientific Reports	2017
Schmidt et al.	Consc Cog	2019
Shekhar & Rahnev	J Neuroscience	2018
Shekhar & Rahnev	PsyArXiv	2020
Sherman et al	Journal of Neuroscience	2016
Sherman et al	Journal of Cognitive Neuroscience	2016
Sherman et al	Unpublished	NA
Sherman et al	Unpublished	NA
Siedlecka, Wereszczywski, Paulewicz, Wierzchon	bioRxiv	2019
Song et al	Consciousness & Cognition	2011
van Boxtel, Orchard, Tsuchiya	bioRxiv	2019
van Boxtel, Orchard, Tsuchiya	bioRxiv	2019
Wierzchon, Paulewicz, Asanowicz, Timmermans & Cleeremans	Consciousness and Cognition	2014
Wierzchon, Anzulewicz, Hobot, Paulewicz & Sackur	Consciousness and Cognition	2019

References

1. Schrödinger, E. *What is Life? The Physical Aspect of the Living Cell.* (Cambridge University Press, 1944).

2. Ashby, W. R. Principles of the self-organizing dynamic system. *Journal of General Psychology* **37**, 125–128 (1947).

3. Friston, K. Life as we know it. *Journal of The Royal Society Interface* **10**, 20130475 (2013).

4. Palva, J. M. *et al.* Roles of multiscale brain activity fluctuations in shaping the variability and dynamics of psychophysical performance. in *Progress in brain research* vol. 193 335–350 (Elsevier B.V., 2011).

5. VanRullen, R. Perceptual Cycles. *Trends in Cognitive Sciences* **20**, 723–735 (2016).

6. Verplanck, W. S. *et al.* Nonindependence of successive responses in measurements of the visual threshold. *Journal of Experimental Psychology* **44**, 273–282 (1952).

7. Atkinson, R. C. A variable sensitivity theory of signal detection. *Psychological Review* **70**, 91–106 (1963).

8. Dehaene, S. Temporal Oscillations in Human Perception. *Psychological Science* **4**, 264–270 (1993).

9. Gilden, D. L. *et al.* On the Nature of Streaks in Signal Detection. *Cognitive Psychology* **28**, 17–64 (1995).

10. Gilden, D. L. *et al.* 1/f noise in human cognition. *Science* **67**, 1837–1839 (1995).

11. Monto, S. *et al.* Very slow EEG fluctuations predict the dynamics of stimulus detection

and oscillation amplitudes in humans. *Journal of Neuroscience* **28**, 8268–8272 (2008).

12. Gilden, D. L. Cognitive emissions of 1/f noise. *Psychological Review* **108**, 33–56 (2001).

13. Duncan, K. *et al.* Memory's Penumbra: Episodic memory decisions induce lingering mnemonic biases. *Science* **337**, 485–487 (2012).

14. Clare Kelly, A. M. *et al.* Competition between functional brain networks mediates behavioral variability. *NeuroImage* **39**, 527–537 (2008).

15. Hesselmann, G. *et al.* Spontaneous local variations in ongoing neural activity bias perceptual decisions. *Proceedings of the National Academy of Sciences of the United States of America* **105**, 10984–10989 (2008).

16. Schroeder, C. E. *et al.* Dynamics of Active Sensing and perceptual selection. *Current Opinion in Neurobiology* **20**, 172–176 (2010).

17. Honey, C. J. *et al.* Switching between internal and external modes: A multiscale learning principle. *Network Neuroscience* **1**, 339–356 (2017).

18. Weilnhammer, V. *et al.* Bistable perception alternates between internal and external modes of sensory processing. *iScience* **24**, (2021).

19. Rahnev, D. *et al.* The Confidence Database. *Nature Human Behaviour* **4**, 317–325 (2020).

20. Aguillon-Rodriguez, V. *et al.* Standardized and reproducible measurement of decision-making in mice. *bioRxiv* 2020.01.17.909838 (2020) doi:10.1101/2020.01.17.909838.

21. Fischer, J. *et al.* Serial dependence in visual perception. *Nat. Neurosci.* **17**, 738–743 (2014).

22. Liberman, A. *et al.* Serial dependence in the perception of faces. *Current Biology* **24**, 2569–2574 (2014).

23. Abrahamyan, A. *et al.* Adaptable history biases in human perceptual decisions. *Proceed-*

ings of the National Academy of Sciences of the United States of America **113**, E3548–E3557 (2016).

24. Cicchini, G. M. *et al.* Compressive mapping of number to space reflects dynamic encoding mechanisms, not static logarithmic transform. *Proceedings of the National Academy of Sciences of the United States of America* **111**, 7867–7872 (2014).

25. Cicchini, G. M. *et al.* Serial dependencies act directly on perception. *Journal of Vision* **17**, (2017).

26. Fritsche, M. *et al.* A bayesian and efficient observer model explains concurrent attractive and repulsive history biases in visual perception. *eLife* **9**, 1–32 (2020).

27. Urai, A. E. *et al.* Pupil-linked arousal is driven by decision uncertainty and alters serial choice bias. *Nature Communications* **8**, (2017).

28. Braun, A. *et al.* Adaptive history biases result from confidence-weighted accumulation of past choices. *Journal of Neuroscience* **38**, 2418–2429 (2018).

29. Bergen, R. S. *et al.* Probabilistic representation in human visual cortex reflects uncertainty in serial decisions. *Journal of Neuroscience* **39**, 8164–8176 (2019).

30. Urai, A. E. *et al.* Choice history biases subsequent evidence accumulation. *eLife* **8**, (2019).

31. Hsu, S. M. *et al.* The roles of preceding stimuli and preceding responses on assimilative and contrastive sequential effects during facial expression perception. *Cognition and Emotion* **34**, 890–905 (2020).

32. Dong, D. W. *et al.* Statistics of natural time-varying images. *Network: Computation in Neural Systems* **6**, 345–358 (1995).

33. Burr, D. *et al.* Vision: Efficient adaptive coding. *Current Biology* **24**, R1096–R1098

(2014).

34. Montroll, E. W. *et al.* On 1/f noise and other distributions with long tails. *Proceedings of the National Academy of Sciences* **79**, 3380–3383 (1982).

35. Bak, P. *et al.* Self-organized criticality: An explanation of the 1/f noise. *Physical Review Letters* **59**, 381–384 (1987).

36. Chialvo, D. R. Emergent complex neural dynamics. *Nature Physics* **6**, 744–750 (2010).

37. Wagenmakers, E. J. *et al.* Estimation and interpretation of 1/fα noise in human cognition. *Psychonomic Bulletin and Review* **11**, 579–615 (2004).

38. Van Orden, G. C. *et al.* Human cognition and 1/f scaling. *Journal of Experimental Psychology: General* **134**, 117–123 (2005).

39. Cicchini, G. M. *et al.* The functional role of serial dependence. *Proceedings of the Royal Society B: Biological Sciences* **285**, (2018).

40. Kiyonaga, A. *et al.* Serial Dependence across Perception, Attention, and Memory. *Trends in Cognitive Sciences* **21**, 493–497 (2017).

41. McGinley, M. J. *et al.* Waking State: Rapid Variations Modulate Neural and Behavioral Responses. *Neuron* **87**, 1143–1161 (2015).

42. Rosenberg, M. *et al.* Sustaining visual attention in the face of distraction: A novel gradual-onset continuous performance task. *Attention, Perception, and Psychophysics* **75**, 426–439 (2013).

43. Zalta, A. *et al.* Natural rhythms of periodic temporal attention. *Nature Communications* **11**, 1–12 (2020).

44. Prado, J. *et al.* Variations of response time in a selective attention task are linked to variations of functional connectivity in the attentional network. *NeuroImage* **54**, 541–549

(2011).

45. St. John-Saaltink, E. *et al.* Serial Dependence in Perceptual Decisions Is Reflected in Activity Patterns in Primary Visual Cortex. *Journal of Neuroscience* **36**, 6186–6192 (2016).

46. Cicchini, G. M. *et al.* Perceptual history propagates down to early levels of sensory analysis. *Current Biology* **31**, 1245–1250.e2 (2021).

47. Kepecs, A. *et al.* Neural correlates, computation and behavioural impact of decision confidence. *Nature* **455**, 227–231 (2008).

48. Fleming, S. M. *et al.* How to measure metacognition. *Frontiers in Human Neuroscience* **8**, 443 (2014).

49. Leys, C. *et al.* Detecting outliers: Do not use standard deviation around the mean, use absolute deviation around the median. *Journal of Experimental Social Psychology* **49**, 764–766 (2013).

50. Maloney, L. T. *et al.* Past trials influence perception of ambiguous motion quartets through pattern completion. *Proceedings of the National Academy of Sciences of the United States of America* **102**, 3164–3169 (2005).

51. Glaze, C. M. *et al.* Normative evidence accumulation in unpredictable environments. *eLife* **4**, (2015).

52. Hermoso-Mendizabal, A. *et al.* Response outcomes gate the impact of expectations on perceptual decisions. *Nature Communications* **11**, 1–13 (2020).

53. Mathys, C. D. *et al.* Uncertainty in perception and the Hierarchical Gaussian Filter. *Frontiers in human neuroscience* **8**, 825 (2014).

54. Sterzer, P. *et al.* The Predictive Coding Account of Psychosis. *Biological Psychiatry* **84**, 634–643 (2018).

55. Rao, R. P. *et al.* Predictive coding in the visual cortex: a functional interpretation of

some extra-classical receptive-field effects. *Nature neuroscience* **2**, 79–87 (1999).

56. Jardri, R. *et al.* Experimental evidence for circular inference in schizophrenia. *Nature Communications* **8**, 14218 (2017).

57. Bengio, Y. *et al.* Towards Biologically Plausible Deep Learning. *bioRxiv* (2015).

58. Dijkstra, N. *et al.* Perceptual reality monitoring: Neural mechanisms dissociating imagination from reality. *PsyArXiv* (2021) doi:10.31234/OSF.IO/ZNGEQ.

59. Andrillon, T. *et al.* Predicting lapses of attention with sleep-like slow waves. *Nature Communications* **12**, 3657 (2021).

60. Passingham, R. E. *Understanding the prefrontal cortex : selective advantage, connectivity, and neural operations.* (Oxford University Press).

61. Bak, P. Complexity and Criticality. in *How nature works* 1–32 (Springer New York, 1996). doi:10.1007/978-1-4757-5426-1_1.

62. Denève, S. *et al.* Efficient codes and balanced networks. *Nature Neuroscience* **19**, 375–382 (2016).

63. Beggs, J. M. *et al.* Neuronal Avalanches in Neocortical Circuits. *Journal of Neuroscience* **23**, 11167–11177 (2003).

64. Wang, X. J. Synaptic basis of cortical persistent activity: The importance of NMDA receptors to working memory. *Journal of Neuroscience* **19**, 9587–9603 (1999).

65. Wang, X. J. Synaptic reverberation underlying mnemonic persistent activity. *Trends in Neurosciences* **24**, 455–463 (2001).

66. Wang, M. *et al.* NMDA Receptors Subserve Persistent Neuronal Firing during Working Memory in Dorsolateral Prefrontal Cortex. *Neuron* **77**, 736–749 (2013).

67. Bliss, D. P. *et al.* Synaptic augmentation in a cortical circuit model reproduces serial

dependence in visual working memory. *PLOS ONE* **12**, e0188927 (2017).

68. Stein, H. *et al.* Reduced serial dependence suggests deficits in synaptic potentiation in anti-NMDAR encephalitis and schizophrenia. *Nature Communications* **11**, 1–11 (2020).

69. Durstewitz, D. *et al.* Neurocomputational Models of Working Memory. *Nature Neuroscience* **3**, 1184–1191 (2000).

70. Seamans, J. K. *et al.* Dopamine D1/D5 receptor modulation of excitatory synaptic inputs to layer V prefrontal cortex neurons. *Proceedings of the National Academy of Sciences of the United States of America* **98**, 301–306 (2001).

71. Kobayashi, T. *et al.* Reproducing Infra-Slow Oscillations with Dopaminergic Modulation. *Scientific Reports* **7**, 1–9 (2017).

72. Chew, B. *et al.* Endogenous fluctuations in the dopaminergic midbrain drive behavioral choice variability. *Proceedings of the National Academy of Sciences of the United States of America* **116**, 18732–18737 (2019).

73. Fritsche, M. *et al.* Opposite Effects of Recent History on Perception and Decision. *Current Biology* **27**, 590–595 (2017).

74. Gekas, N. *et al.* Disambiguating serial effects of multiple timescales. *Journal of Vision* **19**, 1–14 (2019).

75. Weilnhammer, V. *et al.* Psychotic Experiences in Schizophrenia and Sensitivity to Sensory Evidence. *Schizophrenia bulletin* **46**, 927–936 (2020).

76. Fletcher, P. C. *et al.* Perceiving is believing: a Bayesian approach to explaining the positive symptoms of schizophrenia. *Nature reviews. Neuroscience* **10**, 48–58 (2009).

77. Corlett, P. R. *et al.* Hallucinations and Strong Priors. *Tics* **23**, 114–127 (2019).